Steel and Composite Structures, *Vol. 29, No. 1 (2018) 1-22*
DOI: https://doi.org/10.12989/scs.2018.29.1.001

An experimental study of the behaviour of double sided welded plate connections in precast concrete frames

Halil Görgün *

Department of Civil Engineering, Dicle University, 21280, Diyarbakir, Turkey

(*Received January 31, 2018, Revised July 5, 2018, Accepted August 10, 2018*)

Abstract. Multi-storey precast concrete skeletal structures are assembled from individual prefabricated components which are erected on-site using various types of connections. In the current design of these structures, beam-to-column connections are assumed to be pin jointed. Welded plate beam to-column connections have been used in the precast concrete industry for many years. They have many advantages over other jointing methods in component production, quality control, transportation and assembly. However, there is at present limited information concerning their detailed structural behaviour under bending and shear loadings. The experimental work has involved the determination of moment-rotation relationships for semi-rigid precast concrete connections in full scale connection tests. The study reported in this paper was undertaken to clarify the behaviour of such connections under symmetrical vertical loadings. A series of full-scale tests was performed on sample column for which the column geometry and weld arrangements conformed with successful commercial practice. Proprietary hollow core slabs were tied to the beams by tensile reinforcing bars, which also provide the in-plane continuity across the connections. The strength of the connections in the double sided tests was at least 0.84 times the predicted moment of resistance of the composite beam and slab. The secant stiffness of the connections ranged from 0.7 to 3.9 times the flexural stiffness of the attached beam. When the connections were tested without the floor slabs and tie steel, the reduced strength and stiffness were approximately a third and half respectively. This remarkable contribution of the floor strength and stiffness to the flexural capacity of the joint is currently neglected in the design process for precast concrete frames. In general, the double sided connections were found to be more suited to a semi-rigid design approach than the single sided ones. The behaviour of double sided welded plate connection test results are presented in this paper. The behaviour of single sided welded plate connection test results is the subject of another paper.

Keywords: double sided; welded plate; semi-rigid connection; precast concrete frames

1. Introduction

During the past five decades the multi-storey precast concrete structure has developed into an alternative to that of cast in-situ and steel structures. This clearly makes the building market a competitive one.

The present research work focuses on precast concrete structures, where the superstructure is erected from the individual prefabricated components which are made in a factory in a favourable environment and with tight production and quality control. This produces units with high quality performance and appearance. The designer can select from a range of finishes and be able to inspect and accept the units before they leave the factory. Schools, universities and buildings such as hospitals, offices, car parks, hotels are widely being built using precast concrete components.

The very existence of a precast concrete industry and the numerous successful building projects achieved using precast concrete, for the whole or just a part of the structure, is proof that the technique is practical and economical. In global terms, the market share of precast 'grey' frames (structural concrete with no architectural qualities) is probably around 5% of the multi-storey business. However, for precast structures with an integrated facade or other decorative features, the global market share is closer to 15%, being as high as 70% in the colder climates and/or where site labour is expensive (Elliott 2017). Nowadays, with reference to Europe, one-story industrial precast concrete buildings are the most common type to be found at industrial enterprises and constitute 75-80% of total industrial construction (Demartino *et al*. 2017).

Precast concrete offers opportunities for speeding the on-site processes of construction, the maximum re-use of mould work and equipment, and for continuity of the processes. There is a reduction in the amount of in-situ concrete required on-site and reduced delays caused by bad weather and seasonal conditions. Precast allows more accurate programming of the processes of construction and sites using precast concrete structures are typically cleaner.

With all the above advantages, the most economic feature in the precast concrete industry is the standardisation of the products. This has a great influence on the cost effectiveness of the industry. In a typical skeletal precast concrete frame, the different precast concrete components are assembled and interconnected using various

∗Corresponding author, Associate Professor,
E-mail: hgorgun@dicle.edu.tr

http://www.techno-press.org/?journal=scs&subpage=6 ISSN: 1229-9367 (Print), 1598-6233 (Online)

types of connections. The connections may have to transfer forces such as shear, axial, flexure and torsion between the precast components.

Precast skeletal structures are designed either as unbraced structures, up to three or four stories in height, where the stability is provided by frame action of the beams, columns and floor slabs, or as fully braced structures, up to 15 to 20 stories in height, where the stability is provided by shear walls, or columns (Elliott *et al*. 1998).

In both situations the behaviour of the frame in resisting gravity and horizontal load (earthquake or wind) is influenced greatly by the strength, stiffness and ductility of the connections. The stability of an unbraced structure relies entirely on the foundation moment and shear connection because the frame connections at floor levels are currently designed as pinned. In reality, these connections do not behave as pins and therefore the distribution of moments and forces in the frame is not accurately represented in design.

It is therefore important to study the behaviour of these connections together with the effect they have on the overall structure. This experimental work mainly concentrates on the flexural behaviour of beam-to-column connections in the internal, double sided two-way connections, shown schematically in Fig. 1, beam-to-column joints with and without precast concrete hollow core floor slabs and tie steel.

The term "connection" refers to major structural connections between precast components, e.g., welded plate connection. The "joint" includes the connection and where appropriate in-situ concrete, e.g., beam-to-column joint. It is the zone between different adjacent units of a structure.

The stated objectives of the precast concrete programme are to extend the test data available, to use computational techniques to extrapolate the data to a full range of geometries and loading conditions, and to standardise the resulting stiffness measurements in the form of moment-rotation curves for inclusion by design consultants in general frame analysis programmes.

The behaviour of a connection can be properly assessed by experimental testing (Loo and Yao 1995). In terms of codes of practices, ACI 318 (2014), BS 8110 (1985) and EC2 (Eurocode 2 2004) do not facilitate an innovation in precast concrete beam-to-column connections even though the design and analysis of precast structures are significantly affected by their behaviour.

Earthquake resistant reinforced concrete buildings require the structure to resist the induced forces in a ductile manner. This demands that the beam-to-column connections be designed as a ductile, moment-resistant connection. This has severely limited the use of precast concrete construction in seismic zones.

Pillai and Kirk (1981) developed a satisfactory ductile, moment-resistant beam-to-column connection to be used in earthquake resistant buildings with precast reinforced concrete construction. The test results have indicated that the proposed method of connection developed adequate strength, stiffness, and ductility to be classified as a ductile, moment-resistant connection in the context of seismic design. Bhatt and Kirk (1985) grouped moment-resisting connections used for joining precast beam to columns into three categories and carried out tests on the third category on an improved version of the joint detail tested by Pillai and Kirk (1981). Results from the tests have shown that it is possible to achieve highly ductile behaviour by using the joint detail adopted.

Stanton *et al*. (1986) focused on the actual behaviour of commonly used connections. The two programs were combined in order to devote maximum effort to the physical testing of connections in common use. The Research Report (Stanton *et al*. 1986) contains a complete description of the research program, as well as detailed descriptions of the individual tests.

Dolan *et al*. (1987) summarizes the test program. The Research Report along with related publications (Pillai and Kirk 1981, Bhatt and Kirk 1985, Dolan *et al*. 1987, Dolan and Pessiki 1989, Seckin and Fu 1990) began to address a void in the technical literature.

Dolan and Pessiki (1989) demonstrated the feasibility of using models for testing precast concrete connections. Model studies have been examined as an alternative for obtaining basic information about the behaviour of precast concrete connections. The advantages of model studies include lower cost, specimens that are more easily manufactured and handled, a significant reduction in applied loading, and a corresponding reduction in test apparatus size.

Based on a number of considerations, including available materials and available testing frames, a scale of one-quarter was selected for the model studies.

A connection, designated BC-15 in the PCI report "Moment Resistant Connections and Simple Connections" (Stanton *et al*. 1986) was selected for the model. The results have shown that the behaviour characteristics of a welded, monotonically loaded precast concrete connection can be simulated using models.

In Europe, a small number of technical publications and guides on the design of precast wall connections were published, but a lack of information on test data and design models are still missing especially for connections of precast frame structures. The Study and Research Center of the French Precast Industry (CERIB) investigated more deeply in this field. A research programme entitled "Investigation on the behaviour of semi-rigid connections" was divided into two tasks:

- initial classification of connections with respect to their location
- collection of information on tests data and design methods.

Comair and Dardare (1992) carried out a testing programme on thread-rodded connections with grouted sleeves. It was accepted that this connection system is usually viewed as more economical than other systems used in France.

Chefdebien and Dardare (1994) have focused on the behaviour of thread rodded beam column connections within the framework of the design of a three storey two bay building. According to the test results, it has been concluded that the continuity moment on intermediate support could easily be increased to a value equal to 30% of the bending moment of a simply supported beam.

Mahdi (1992) carried out fourteen tests to evaluate experimentally the degree of semi-rigidity afforded by the most common types of beam-to-column connections used in the precast concrete industry in the U.K. It has been observed that all connections possessed some strength and stiffness, but the capacities varied over a wide range, i.e., from 5 to 210 kNm, and stiffness from 200 to 19,000 kNm/rad.

Virdi and Ragupathy (1992) conducted eight tests on precast concrete sub-frames to provide data for the validation of computational results. Each sub-frame consisted of a 6 m long continuous column together with a stub length (2 m) of the beam. It has been reported that results for the tests show good correlation. By comparing the slopes of the beam and column at the beam column junction, it has been possible to deduce the moment rotation characteristic of the particular connection.

Mohamed and Jolly (1995) conducted two full-scale test programmes on sleeved bolt connections. Joint moment stiffness has been characterized by the moment-rotation curves. These curves show that the number of bolts per joint has an effect on the joint's rotational rigidity.

Loo and Yao (1995) investigated the strength and deformation behaviour of two types of precast reinforced concrete beam-to-column connections. A total of 18 half-scale interior connection models were designed, built, and tested to failure to evaluate their strength and ductility properties under static and unidirectional repeated loading. They include four monolithic models and four each of the precast connection Types A and B static load tests. From the results, it was concluded that all the precast models possessed not only greater ductility but also higher stiffness than their monolithic counterparts.

Cheok and Lew (1991, 1993) tried to develop seismic resistant precast concrete beam-to-column connections using experimental tests. They studied the connections in terms of strength, ductility and energy dissipation characteristics.

Cheok *et al*. (1998) analysed moment-resisting precast concrete frames with hybrid connections under seismic loads to develop a design guide for precast concrete hybrid connections in regions of high seismicity using the results of frames analyses and previous experimental tests.

Englekrik (1995) tried to develop a ductile beam-to-column connection to be employed in a moment resisting frame. The experimental tests conducted showed that the proposed beam-to-column connection performance was better than cast-in-place and structural steel systems under cyclic loading.

Various research works were conducted on precast concrete beam-to-column connections by Elliott *et al*. (2003a, b). Considering the fact that the precast concrete beam-to-column connections behave as semi-rigid connections, they proposed that the global precast frame can be designed semi-continuously. This semi-rigidity assumption may result in more economical design in comparison with pinned connections depending of the degree of semi rigidity of the connection.

Khaloo and Parastesh (2003) carried out an experimental on five precast concrete beam-to-column and one monolithic connection. As a result, the authors concluded that the precast concrete connections provided strength, ductility and energy dissipation capacity comparable to their monolithic counterparts.

Ertas *et al*. (2006) experimentally tested several beam-to-column connections and compared with the monolithic connections. Stiffness, strength, ductility and energy dissipation were the bases of the comparison.

Full-scale experimental investigation was reported by performing and comparing full-scale tests on precast concrete and monolithic H-shape sub-frames (Rahman *et al*. 2007). In addition, as a result of load-displacement curves of mid-span the precast connection showed a better structural performance than reinforced concrete specimen.

Kulkarni and Li (2009) reported that although the research studies done on hybrid steel-concrete beam-to-column connections with cast-in-place are few, the literature related to hybrid precast concrete joints is rare.

A new hybrid steel-concrete beam-to-column connection through nonlinear finite element method and four experimental tests was investigated by Kulkarni and Li (2009), Kulkarni *et al*. (2008) and Li *et al*. (2009). They concluded that the high flexibility in the beam-to-column joint of the precast concrete specimens causes higher rotation of the precast beams compared with the cast-in-place concrete specimen.

Kwong and Teng (2000) reported the results of their experimental work on eight precast concrete beams using a hybrid connection consists of I-steel and concrete. They investigated the effect of stirrup spacing and embedded lengths of the I-steel on the failure load of hybrid beams with hinge supports.

A hybrid precast steel-concrete beam system incorporating an H-steel and a reinforced concrete beam is studied through three test specimens (Yang *et al*. 2010). It was concluded that the flexural behaviour of the hybrid precast beam was improved significantly by adding the longitudinal prestressing tension force.

Moghadasi and Marsono (2012) investigated the crack pattern, modes of failure, ultimate strength and ductility parameters of an Industrialised Building System (IBS) beam-to-column connection, and compared with conventional reinforced concrete during the load-displacement analysis.

It has been reported that the dowel type of the connection is the most common all around the world (Kataoka *et al*. 2015). However, the knowledge about its seismic behavior was incomplete and poorly understood. To analyze the failure of dowel mechanism, Zoubek *et al*. (2013) created a numerical model in the FEA software and calibrated using the results of the experimental investigations. In Choi *et al*. (2013), a typology of beam-column connections using steel shapes as steel connector was tested. The shapes were casted with the structural elements (column and beam) and they are used to carry out the connections by bolts. In this type of connections there is

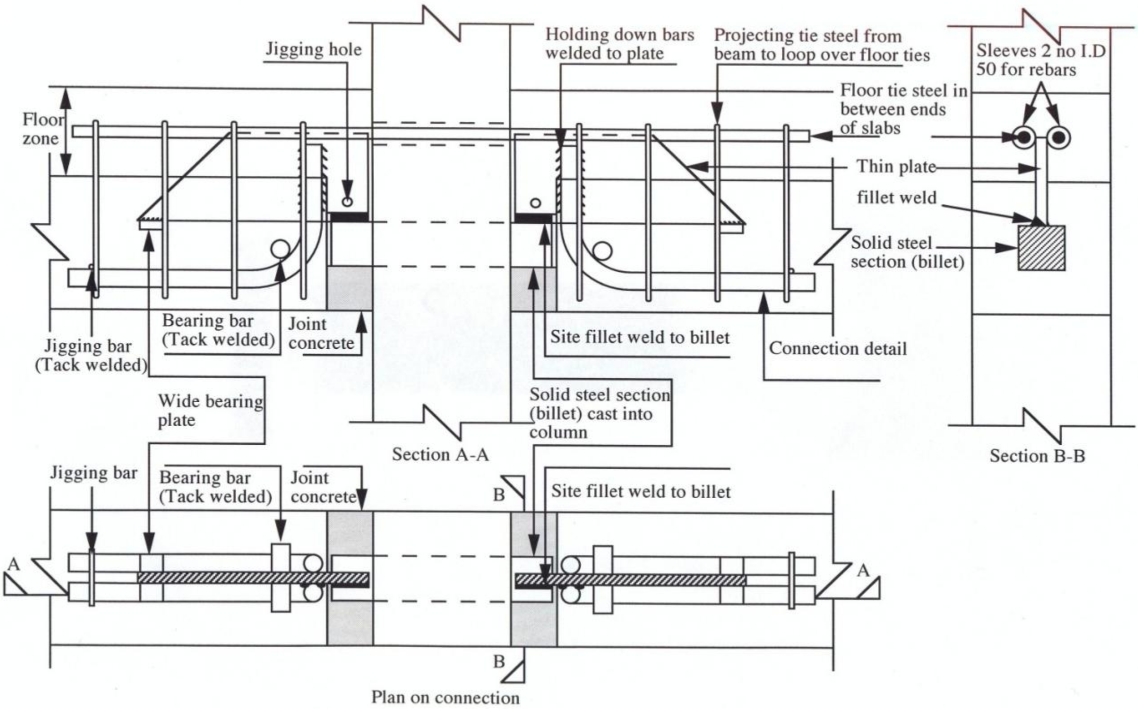

Fig. 1 Welded plate and billet beam-to-column connection (two way connection)

not the presence of corbels and dowels.

Kataoka *et al.* (2015) investigated the behavior of a specific type of beam-column connection composed of concrete corbels, dowels and continuity bars passing through the column. The study was developed based on the experimental and numerical results. The comparison of the results showed a satisfactory correlation between loading versus displacement curves.

Marsono *et al.* (2015) investigated the structural performance of an IBS beam in nonlinear state through load-displacement relationship of beam, crack pattern, mode of failure, stresses at concrete and connection deformation.

Moghadasi *et al.* (2017) conducted two full-scale experimental tests on rotational behaviour of a new innovated hybrid steel-concrete Industrialised Building System (IBS) beam-to-column connection patented as Smart IBS. The rotational stiffness and ductility were investigated through load-rotation curves. In addition, the degree of rotational rigidity of the connection in different rounds of loading was investigated.

Welded plate connections, shown in Fig. 1, are among the most extensively used. Their advantages and disadvantages can be found in details in Görgün (1997).

In this paper, rotational behaviour of welded plate and billet beam-to-column connections (two-way connections) is investigated by conducting full-scale experimental test. They have many advantages over other jointing methods in component production, quality control, transportation and assembly. However, there is at present limited information concerning their detailed structural behaviour under bending and shear loadings. The experimental work has involved the determination of moment-rotation relationships for semi-rigid precast concrete connections in full scale connection tests. The rotational stiffness and ductility were investigated through moment-rotation curves. In addition, the degree of rotational rigidity of the connection in different cycles of loading was investigated.

2. Precast concrete beam-to-column connections

In the UK the most popular type of precast concrete connection is known as the “hidden corbel” because the main structural components cannot be seen on completion. This has the advantage of minimising the depth of the connection and protecting all structural steel and rebars in the concreted or grouted joint. The two main variations of the hidden corbel are:

- welded plate and billet beam-to-column connection.
- bolted billet beam-to-column connection.

A billet is the name given to any projecting steel member, such as solid section, rolled hollow section (RHS) etc. The space reserved for the site operations immediately beneath the billet is concreted or grouted solid on-site using either concrete containing small sized (6-10 mm) aggregates, or sand-cement grout. Expanding agents (or expansive cements) are used to ensure that no shrinkage cracks allow ingress of reactive substances along the construction joints. The size of the infill depends on the type and the shear capacity of the particular connection, but in the main is 100 to 150 mm × 100 to 200 mm deep. The breadth of the infill may either be equal to the breadth of the beam, or in the case of very wide beams may be equal to the breadth of a pocket. In either case the breadth of the infill will be about 300 mm.

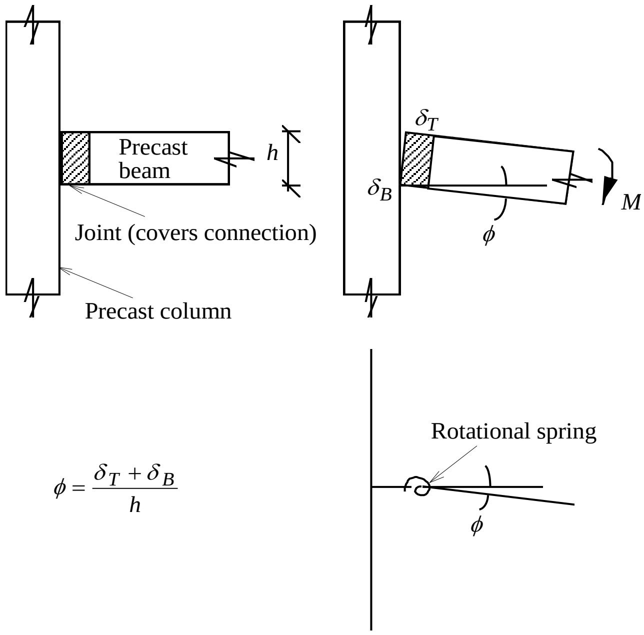

Fig. 2 Simplified definition of joint rotation

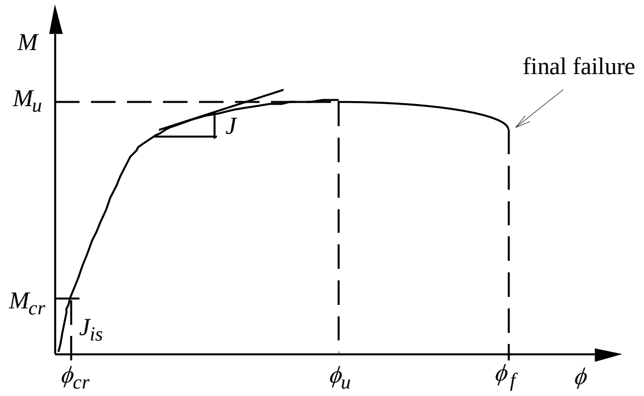

ϕ = relative joint rotation (rad)
J_{is}= initial secant rotational stiffness (kNm/rad)

Fig. 3 Moment-rotation characteristic

3. Properties of beam-to-column connections

3.1 Fundamental response

The connections in precast concrete frames are subjected to both clockwise and anti-clockwise bending moments M and this induces the relative rotations ϕ between the beam end and the adjacent column as shown in Fig. 2.

Connections such as these are known as "semi-rigid". Total frame analysis may therefore be carried out by substituting rigid joint connections with ones of finite strength, rotational stiffness and ductility. The relevant properties of connections are strength, stiffness and deformation capacity (ductility). The behaviour may be described in terms of the well-known moment-rotation M-ϕ data, idealised in Fig. 3, but in the case of precast concrete connections the semi rigidity is due to both material and large deflection effects. There is also a zone of influence beyond the immediate locality of the joint. Previous and new work has shown that this is approximately equal to the cross sectional dimensions of the adjoining beam and column members (Mahdi 1992). In this context it is very important that the M-ϕ characteristics of the connection are tailored to suit the stiffness and strength of the frame.

It is thought that the initial rotational stiffness J_{is} in Fig. 3 of the connection is due mainly to the geometry of the joint, in particular in the manner in which it is constructed and the tolerances made for lack of fit etc. on-site. This is particularly relevant in grouted and bolted joints where slippage may take place at low loads and give an artificially low stiffness. On the other hand, the ultimate strength of the connection M_u in Fig. 3 is due mainly to the strength of the critical materials in the joints, i.e., the crushing and shear strength of the concrete and the yield and tensile strengths of the reinforcements. Finally, the ductility of the connection is mainly a function of the ductility of the reinforcement, but geometry plays a large part in this, particularly if the connection is over reinforced. If normative rules are to be developed to classify such connections, the geometric and material effects must be separated and accounted for in any single M-ϕ plot, where the general rotational stiffness J of the connection is given by the gradient of the M-ϕ curve as shown in Fig. 3.

The usual approach is to express stiffness as a non-dimensional term K_s where

$$K_s = \frac{J}{4E_c I/L} \tag{1}$$

i.e., the ratio of the stiffness of the connection, J, to the flexural stiffness of the beam,$4E_cI/L$, to which it is attached, where E_c is the modulus of elasticity of concrete, I is the second moment of inertia of uncrushed section of the beam, and L is the effective span of the beam.

3.2 Classification of beam-to-column connections

Depending on which criterion for frame analysis is used, i.e., sway stiffness, column buckling load etc., these connections may fall into one of three classes, namely

- Class 1. rigid with full strength
- Class 2. semi-rigid with full or partial strength
- Class 3. pinned

In the case of precast connections, the important classification boundary is the one, which separates Classes 2 and 3.

It is well known that the actual response of almost all beam-to-column structural connections is non-linear. The concept of a perfectly rigid or pinned connection is a purely theoretical one but useful to the designer to simplify the calculation of framed structures.

In engineering calculations, some actual beam-to-column connections can yet be considered as pinned or perfectly rigid if their behaviour is such that the bending moment they can carry over is so low, and the relative rotation between the connected beam and column is not large enough, respectively, to significantly influence the overall behaviour of the frame.

Several classification systems for beam-to-column connections in steel frames have so far been proposed in order to determine whether an actual beam-to-column connection can reasonably be considered as pinned or semi-rigid (where the joint flexibility has to be taken into account) or rigid in the frame design stage. Details of these classification systems are given in Görgün (1997).

3.3 Simplified component method

The definitions used in this work are that the connection moment M_{con} is measured in the joint at the face of the column, and ϕ is the relative rotation of the beam to the column at the same point. Thus assuming that the end of the beam of overall depth h acts as a rigid body, beam end rotations may also be expressed as follows. Refer to Fig. 2

$$\phi = \frac{\delta_T + \delta_B}{h} \tag{2}$$

where δ_T is the crack opening plus other linear displacements in the concrete at the top of the joint, and δ_B is the compressive deformation in the concrete at the bottom of the joint. Thus if δ_T and δ_B can be computed separately for given loading and expressed in terms of material and geometric properties, a simple method to determine ϕ is possible. In this method an "effective modulus of elasticity of concrete E_{ce}" is found by experimentation and the associated strains, and hence deformations δ_B, are determined from the appropriate state of stress. Similarly, in the tension zone an "effective tensile stiffness K_e" is found which relates bond and tensile deformation $\delta_T$to the applied tension forces. Experimental testing has been carried out to measure these values, which may then be validated against the results of full connection assembly tests. These tests are referred to as "interface tests" in Görgün (1997).

4. Advantages of using semi-rigid connections

Obviously, the flexural stiffness, bending moment and the deformation capacity (ductility) of semi-rigid beam-to-column connections in any type of structure, either precast, steel or composite, influence greatly the response of the structure as a whole. The general advantages of using semi-rigid connections depend on the type of frame and the usual basis of design. For braced frames this is simple construction, assuming pinned connections, for unbraced frames this is continuous construction, assuming rigid connections.

For braced frames, the effect of semi-rigid connections on beam design can be observed by investigating the behaviour of a single span beam. Fig. 4(a) shows a simply supported beam, with a uniformly distributed load, the maximum design bending moment takes place at mid-span of the beam. In Fig. 4(b) the simple supports have been replaced by fixed supports. Now, the maximum elastic bending moment takes place at the fixed supports, and is two-thirds of the maximum elastic bending moment of the simply supported case.

Fig. 4(c) shows a beam with semi-rigid end connections. Based on the flexural stiffness of the connection, the maximum elastic bending moment occurs at the supports or at mid-span (assuming the semi-rigid end connections have the same flexural stiffness capacity), but will always be less than that for a simply supported and/or fixed supports beam, and permit a reduction in the beam material. The optimum connections would be those which would allow just enough end rotation to balance end and mid-span moments. Semi-rigid connection theory is concerned with this problem and other, similar matters.

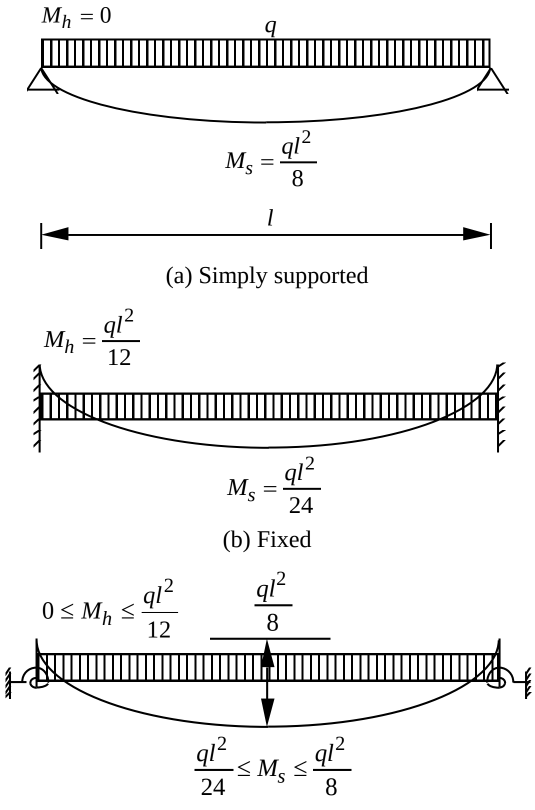

Fig. 4 Beam moments with various end conditions

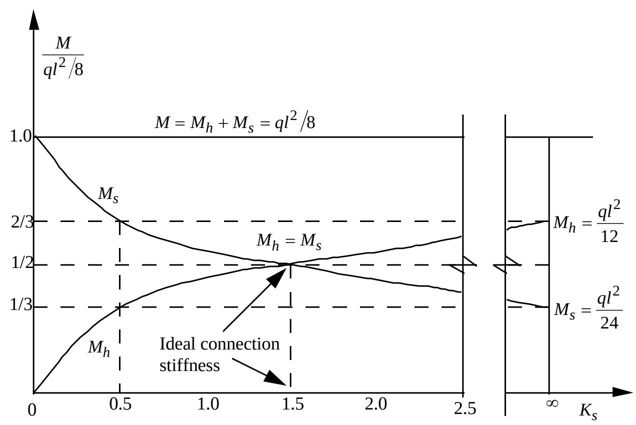

Fig. 5 Variation of beam moments with connection stiffness

Fig. 5 shows that by an appropriate choice of connection stiffness relative to the beam K_s, the elastic bending moment at the supports can theoretically be made equal to the value at mid-span, hence minimizing the elastic design moment. Of course, there may well be practical difficulties however in providing such a precise flexural stiffness value. Such a solution may not be the optimum. This is because of the additional cost of providing connections with the required flexural stiffness. Fig. 5 shows that the design moment is significantly reduced even if the stiffness of the connection is only modest. This also means that a small reduction in the stiffness of the connections will have a dramatic effect on the design moment of the beam.

A similar pattern occurs when the elastic mid-span deflection of the beam is considered. The variation in the elastic mid-span deflection of the beam with end conditions and connection stiffness can be seen from Figs. 6-7. It has been suggested that reduced beam depth (Anderson *et al*. 1993) can economically be obtained by either:

- recognising the inherent stiffness of some types of simple connection, or
- modifying simple connections to a limited extent to provide increased stiffness.

One of the objectives of this study has been to recognise the inherent flexural stiffness and strength of the beam-to-column connections as used in precast concrete structures in the UK and to incorporate this into design procedures rather than to modify the connections.

5. Evaluation of semi-rigid connections using beam-line method

For braced frames, the beam-line concept shown in Fig. 8 provides a convenient method to determine the influence of semi-rigid connections on the behaviour of an elastic beam in one interactive process. This approach in effect combines characterization of connection response, analysis

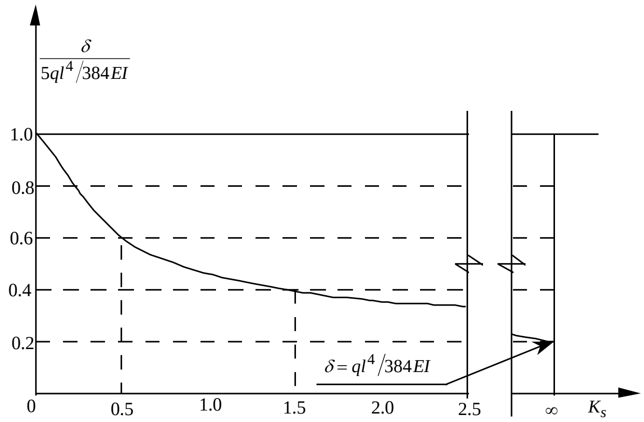

Fig. 6 Variation of mid-span deflection with connection stiffness

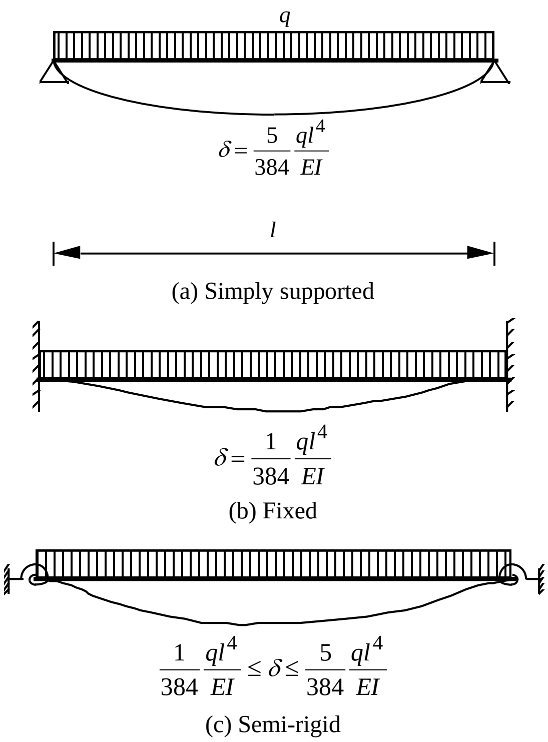

Fig. 7 Beam deflected profiles with various end conditions

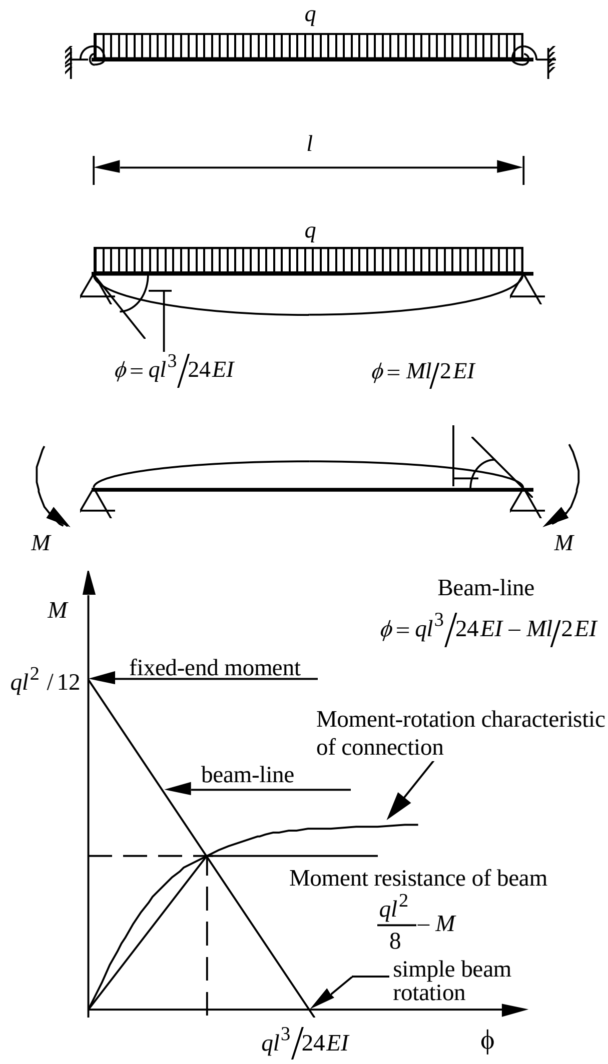

Fig. 8 Definition of beam-line

of internal moments, and evaluation of performance. Using this method, connection characteristics may be tested by being superimposed on the beam-line to determine the corresponding values of end moment, and thereby the beam design moment. Alternatively, the minimum connection stiffness needed to justify a particular beam section can be determined. This approach leads directly to the minimum connection resistance needed to achieve the elastic connection behaviour assumed in the analysis. Full details of the beam-line method have been described by Elliott *et al*. (2003a, b).

6. Objectives of the work

(1) To provide actual moment-rotation characteristics of two types of beam-to-column connections experimentally, incorporated in double and single sided sub-frames
(2) To obtain the moment-rotation characteristics of the connections from smaller isolated joint components tests
(3) To present a method of application of the moment-rotation characteristics of the connections in the analysis and design of multi-storey precast concrete framed structures

These objectives have been realised practically on the basis of the following experimental work:

(1) Full scale frame connection tests on:
- welded plate and billet beam-to-column connection
  - (a) Double sided beam-to-column connection (two-way connection) with and without hollow core floor slabs and floor tie steel
  - (b) Single sided beam-to-column connection (three-way connection) with hollow core floor slabs and floor tie steel
- bolted billet beam-to-column connection
  - (a) Double sided beam-to-column connection (two-way connection) with hollow core floor slabs (in-situ concrete only in some tests) and floor tie steel
  - (b) Single sided beam-to-column connection (three-way connection) with hollow core floor slabs and floor tie steel

(2) Interface tests on:
  - (a) Small scale precast-in-situ-precast interfaces in compression and flexure
  - (b) Full scale precast-in-situ-precast interfaces in bond slip and bond failure of re-bars in narrow in-situ concrete strips.

The experimental study of double sided welded plate and billet beam-to-column connection (two way connection) shown in Fig. 1 with hollow core floor slabs and floor tie steel is the subject of this paper.

7. Experimental programme for full scale frame connection tests

The main aim in the full scale precast concrete frame connection tests is the determination of the moment-rotation M-ϕ characteristics of the most common types of beam-to-column connections used in the precast concrete frames in the UK as shown in Fig. 1. From these characteristics it will be possible to abstract the rotational stiffness, bending strength and ductility of the corresponding connections and hence their effects on the stability of these frames. Because currently, beam connections are rated and identified by their shear capacity only, a shear test TW1(B) was carried out after the bending test TW1(A) was completed to ensure that the shear resistance of the entire connection was satisfactory.

In this project study, it is hoped that the connections can be identified not only by their shear capacity but also by their rotational stiffness, flexural strength as well as ductility.

The contribution of these main characteristics of the connections (also referred to as joints on completion) to frame behaviour under gravity cycling loading is well studied in braced (non-sway) precast concrete frames where the precast concrete connections are subjected to hogging bending moments. For this reason, braced frames were considered in the present study.

The joints in braced frames may be classified according to their locations, as those required to connect beams to internal columns and those required to connect beams to external columns. Therefore, two separate investigations are required on internal and external sub-frames.

The length of the beams, and hence the position of the bending load P was selected to represent the point of contra-flexure in a uniformly distributed loaded beam. Assuming that the maximum bending moment is recorded at the face of the column, the shear span / beam effective depth ratio for the load is 2365 / 400 = 5.91. The effective depth to the reinforcement, 2T25 tie bars, is 500 – 100 = 400 mm. The lever arm distance at 2.365 m was kept constant, even though it will change when plasticity is reached in the connection. The sub-frame, connect beams to internal columns, (essentially symmetrical) was simulated in test series 1, with and without the precast concrete proprietary slip formed hollow core floor slabs (supplied by Bison Floors, UK). This was done in order to investigate the influence of incorporating the floor slabs on the main properties of the connections in a double sided precast concrete connections shown in Fig. 1. As can be seen the overall dimensions of these sub-frames indicate that they are full scale tests. It is important to have full scale test data for each of the connections shown in Fig. 1 to compare with those derived from the isolated joint tests, and to be able to predict the behaviour of a number of full scale frame connections from the isolated joint tests reported in Görgün (1997).

Test series 1 included three tests (TW1(A), TW1(B) and TW1(C)) on double sided full scale (internal) sub-frame assemblages with floor slabs (TW1(A) and TW1(B)) and without floor slabs (TW1(C)) and incorporating two way welded plate connection (Fig. 1 and Table 1).

Table 1 Schedule of full-scale frame connection tests

Test series	Test reference	Connection type	Sub-frame type	Floor slab
1	TW1(A)	Welded plate	Double sided	Hollow core
	TW1(B)	Welded plate	Double sided	Hollow core
	TW1(C)	Welded plate	Double sided	None

In the tests, the sub-frames were subjected to vertically applied bending loads at the free end of the precast concrete cantilever beams in an attempt to simulate the pattern of gravity loading. A shear test TW1(B) was also carried out. The frames consisted of continuous 300 × 300 mm columns, 300 × 300 mm beams spanning in *x*-direction, and 200 mm deep hollow core floor slabs spanning at right angles to the beams. The in-situ concrete infill placed over the top of the beams gives a composite floor beam section 500 mm deep. The compressive cube strength for the precast beam, column and beam-to-column joint concrete and grout is specified as 40 N/mm^2 for the slab as 60 N/mm^2, and for in-situ concrete infill over the top of the beams as 30 N/mm^2.

7.1 Details of beam-to-column connections

The beam-to-column connections that use steel inserts at the beam end and at the column to transfer load are considered in three parts (I Struct E, 1978):-

- as a column insert alone, transferring load to the concrete of the column
- as a beam-end detail, transferring load from the concrete of the beam, and
- as a totality, with inserts from the beam and column joined together, and the joint completed

The way in which the connection is assembled and completed affects the choice of inserts. Methods of calculation for some of the more commonly used inserts are given in the I Struct E Manual (1978). In most cases beam shear force is transferred through direct bearing between the inserts.

The welded plate and billet beam-to-column connection (to be referred to as welded plate connection) used in this project study (see Fig. 1) uses a 25 mm thick, cast in mild steel, narrow beam connection plate (the ISE, 1978: Narrow beam plates Type III) projecting from the end of the beam and a projecting wide section solid steel billet insert embedded in the column (see Fig. 9).

The design method is used where the projecting plate cannot be fully contained in the depth of the beam (see Fig. 1). Typical applications are in the ends of the precast parts of composite beams. It is located on the vertical centre-line of the beam. Shear reinforcement in the beam is carried through to the end of the beam so that the insert is well contained by links. The links project above the precast

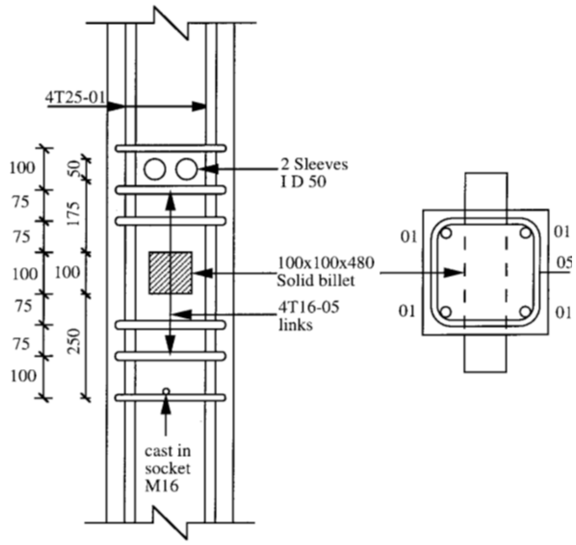

Fig. 9 Reinforcement details in the column around the billet (front elevation)

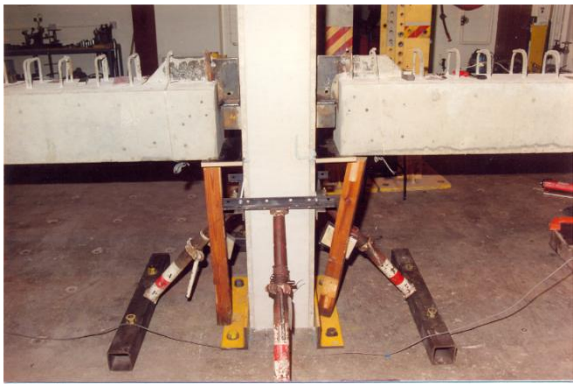

Fig. 10 Welded plate connections after welding

section, and the precast beam is propped until its in-situ topping has reached an adequate strength. The main tension bars in the beam are taken through to the end of the beam and adequately connected to the plate anchor bars by special links. The beam end plate bears on the projecting wide section solid billet in the column and is welded using 20 mm fillet weld (see Fig. 10).

Welding the steel inserts requires skilled labour and is a special operation to ensure that weld cooling does not cause permanent twist in the precast members.

The connection (the 100 mm gap between beam and column) is subsequently filled up to the top level of the beam with nominal $f_{cu} = 40\,\mathrm{N/mm^2}$ strength in-situ concrete using 10 mm aggregate without additives and is now called a joint.

7.2 Design and manufacture of precast concrete test components

Geometric and reinforcement details of the column, around the billets are presented in Fig**.** 9. The column size 300 × 300 mm was used throughout the experimental work. This is the minimum size required to accommodate the types of wide section column inserts under investigation. Other provisions in the column were sleeves to allow the passage of continuing longitudinal reinforcement, and two M16 dia, cast-in sockets to facilitate fixing the instrumentation. The column reinforcement contained 4T25 main bars and T12 links @ 185 mm c/c. The design ultimate axial capacity of a short column with zero moment was 2085 kN for $f_{cu} = 40\,\text{N/mm}^2$ and $f_y = 460\,\text{N/mm}^2$.

Geometrical and reinforcement details of the beams for welded plate and billet connections are presented in Fig. 1. The ends of the beams connected to both sides of the column vary in accordance with the requirement of casting in a standard beam connection plate of 278 kN (Bison literature reference K/278/ Fig. 1) design ultimate shear capacityfor welded plate and billet connections. The beams are considered as acting compositely with the floor slabs and contained 4T20 bars, top and bottom, and T10 shear links @ 100 mm c/c. Design ultimate moment of resistance of the composite beams were 241.10 kNm ($f_y = 460\,\text{N/mm}^2$, $f_{cu} = 40\,\text{N/mm}^2$, partial safety factors for strength γ_m: ultimate limit state taken as 1.15 and 1.50 for reinforcement and concrete respectively, using BS 8110 simplified stress block). The design ultimate ($\gamma_m = 1.25$) and calculated ultimate ($\gamma_m = 1.0$) shear resistance were 250 and 312.5 kN, respectively

The slab units were 1200 mm nominal width by 200 mm depth and 1000 mm long precast prestressed hollow core units (Roth type), each of which contained cut outs (see Fig. 12) to permit the placement of reinforced (T12 transverse bars) in-situ concrete infill. The thickness 200 mm of the slabs represents the most widely used thickness in precast concrete structures. The slab units contained 33 no. 5 mm diameter crimped prestressed wires. The ultimate design sagging moment and shear resistance of the slabs were 125.6 kNm and 162.10 kN, respectively (Bison literature reference).

The experimental specimens mentioned in this study are as same as the author's PhD thesis (Görgün 1997).

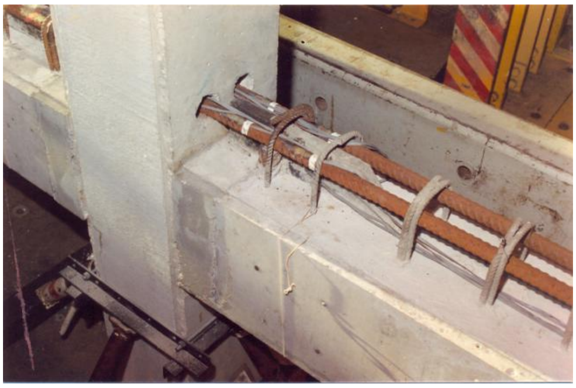

Fig. 11 Location of stability tie bars with steel strain gauges (Görgün 1997)

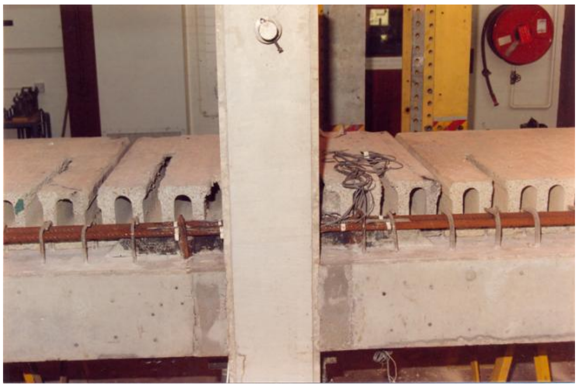

Fig. 12 Sub-frame under construction

7.3 Horizontal ties for building integrity

The specific requirements relating to ties in precast concrete structures are given in BS 8110, Part 1, clause 5.1.8. Tie passing through precast columns (double sided tests, see Fig. 11) are fed through oversized sleeves (usually two to three times the diameter of the tie bars) and later concreted in. The tie steel is implicitly provided for precast frame stability, and not for the sole purpose of these tests.

The tie steel was designed according to BS 8110, Part 1, clause 3.12.3.4.2 assuming that the structure was 5 stories in height, and the floor dead (g_k) and live (q_k) loads were each 5.0 kN/m^2, respectively. The spans for the beam and slabs were both taken as 6 m.

7.4 Concrete mixes

10 mm single-sized Trent River Valley coarse (gravel) uncrushed aggregate were used in all the test carried out. The fine aggregate consisted of uncrushed sand complying to medium grading zone. Ordinary Portland cement complied with the standard requirements was used in all the tests. The correct quantities of cement, aggregates and water were batched and mixed using a 0.1 m^3 capacity laboratory mixer.

7.5 Test rig

A test rig (Fig. 13) was designed according to BS 5950: 1985 to accommodate the test sub-frames. The rig consists of two parallel tie back steel frames aligned perpendicular to the test sub-frames. Both of the tie back frames are capable of carrying 600 kN working load at the centre of the horizontal 250×150×16 RHS cross beam between two 152×76×10 channel-stanchions. This was calculated on the basis of the available number of the holding down bolts. Vertical bending loads at the free ends of the concrete cantilever beams of the test sub-frames were applied incrementally through hand operated hydraulic jacks and measured using 200 kN capacity electrical resistance load cells. The jacks were clamped to the cross beams as shown in Fig. 14. The beams were loaded so as to provide in-plane bending only and to keep the continuous column in a vertical plane. This induced the correct bending moments and shear forces in the connections by keeping the lever arm constant.

Two semi-roller load spreaders were used underneath the load cells to make sure that the positions of the applied loads were kept constant.

Two 100 kN capacity load cells were also positioned

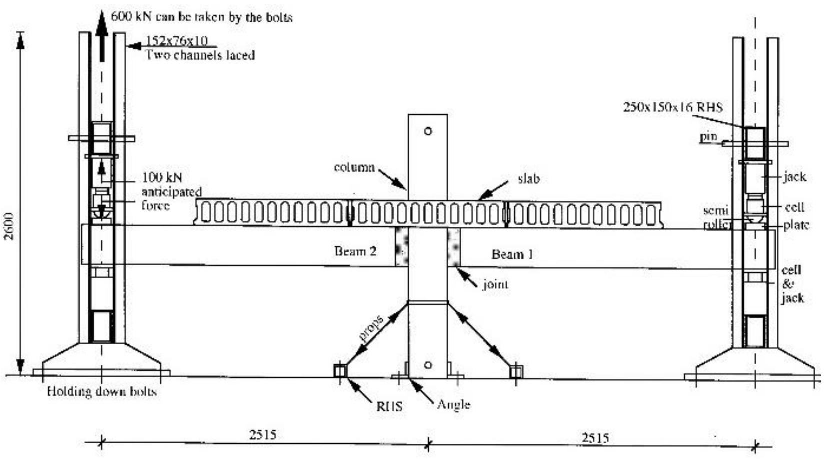

Fig. 13 Front elevation of test rig with sub-frame

Fig. 14 Mechanisms at the free ends of the beams

beneath the end of the beams as shown in Fig. 14 and used to measure the self-weight of the test components in order to find out the initial bending moment of the connections due to self-weight.

7.6 Test procedure

The column was lifted vertically using a crane and a pin passing through the top sleeve of the column. It was placed on to the strong laboratory floor on smooth casting face. It was decided to cast the bottom face of the column as smooth as possible before casting. The length of the mould available in the laboratory was longer than the required overall height of the column by 400 mm. A 25 mm thick timber plate was used between the free end of the mould and the top of the column. This end could be move during casting and vibrating the fresh concrete. Thus, one of the ends of the mould was chosen as reference for the bottom face of the column to make sure that this face is smooth enough to keep the column in its vertical position after erecting.

The column was permanently braced against in and out of plane movements to ensure stability during the replacement of the beams and slab units. The bracing used two 630 mm long 120×120×16 angles, four 690 mm long “Acrow SGB” props (two for each plane). Four 100×100×5×900 mm long RHS were used to support the props to transfer their loads acting on to the laboratory floor.

The beams were placed at one end on the column connection and at the other were seated on to a timber plate support were placed on to the load cell. The load cell was supported by a large travel hydraulic jack to lift the free end of the beam into the correct horizontal position (see Fig. 14) before welding the ends of the beam unclamped to prevent twisting during the welding of welded plate connections. The beam connections were welded to the column connections using the fillet weld (NOVOF IL 70 SG2, 1.2 mm wire) made using covered electrodes complying with BS 639 and steel complying with BS 4360 for mild steel. (It was carried out by a professional welder from the Engineering Faculty Workshop). The welding was done slowly to prevent twisting because of high temperature during the welding. After each layer of weld, it was left to cool before for the next run. Fig. 10 shows the welding region of the connections. Beam 2 had a 5 mm initial twisting (out of plane) before welding. The imperfections were re-measured after welding, and the maximum imperfections (twisting) were about 7 and 8 mm for the beams 1 and 2, respectively. The throat thicknesses and the leg lengths welds were measured using weld measuring apparatus and a small steel ruler in the narrow connection regions.

During joint concreting or grouting, the ends of the beams seated on to the billets projecting from the column face were held providing timber formwork for both sides of the column (for double sided connections) and were clamped using large G clamps for welded plate and billet

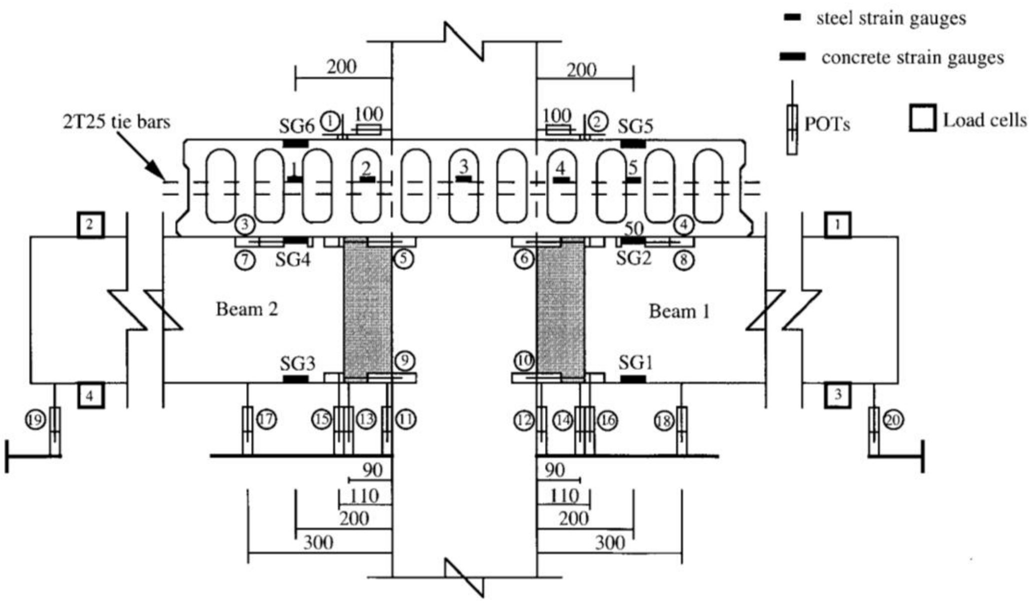

Fig. 17 Instrumentation

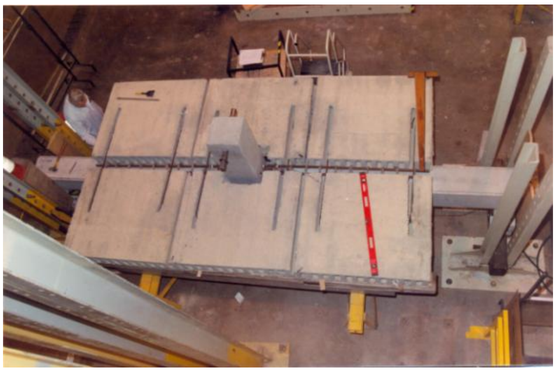

Fig. 15 Sub-frame ready to cast slab-beam-column in situ concrete

Fig. 16 General assembly in structures laboratory for test

connections.

The beam-to-column joints were concreted without vibrating, but tamped carefully.

Two plastic tube sleeves passing through the column were removed and 2T25 (grade 460) longitudinal tie bars (bar A and bar B) with steel strain gauges on were passed through the open sleeves and were placed over the beams. The bars were tied to the shear links projecting from the beams. New measurements were taken after positioning the bars, i.e., centre distance of the bars from the top of the beams. It was not possible to measure from the top of the beams. Owing to some casting problems the top edges of the beam had a 25 mm wide rebate, which reduced the bearing distance between the slab units and the beams from 75 mm to 50 mm. The bottom edges of the beams were used as reference points to measure the distances required. Fig. 11 shows the location of the 2T25 tie bars and steel strain gauges.

Trestles, timber shims and a RHS cross beam were provided to support the slab units temporarily. These units were then seated at one end on to the beams with a bearing distance of 50 mm and the remote end on to the timber shims that were placed on the top of the RHS cross beam seated on to the trestles (see Fig. 12). The horizontal position of the slab units was adjusted using small timber packs. The ends of the slab-to-slab joints and sides of the column at the bottom level of the slabs were moulded to cast slab-beam-column in-situ concrete.

The transverse reinforcement as placed into the opened cores of the slabs is shown in Fig. 15.

The construction was completed filling the gaps between the slabs, over the top of the beams and around the column using the slab-beam-column in-situ concrete. The entire sub-frame was then coated with a brittle white wash coat to detect the formatting cracks (Fig. 16). Testing dates were determined by the cube strength of the in-situ concrete.

The same general procedure was followed for the remainder of the tests.

7.7 Instrumentation and measurement

Fig. 17 presents the layout of the different measuring instruments that were used in tests

The important measurements were:

(a) Vertical deflections of the beams
(b) Crack width δ_T at boundaries of the slab, beam and column
(c) Compressive deformation δ_B in the compression zone
(d) Strain in the tie bars in the tension zone
(e) Strain in the concrete in the compression zone

For one of the main tests twenty deflection transducers (potentiometric type), called "POTs", were used to measure the vertical deflections, crack width and compressive deformation. All of the offsets were measured at the beginning of each test after the attachments of the POTs were completed.

Six 30 mm concrete strain gauges (type: PL - 30-11, gauge resist: 120 ± 3 Ω, gauge factor: 2.12) and ten 10 mm steel strain gauges (type: FLA - 10-11, gauge resist: 120 ± 3 Ω, gauge factor: 2.13) as shown in Fig. 17 were used to record the strains.

All signals from the sensors were automatically recorded using a model data logger. The signals were then linearized by inputting the respective calibration factors (the load cells were calibrated before carrying out the tests) for the various sensors into the data logger and the results were displayed directly in the units of mm for POTs and kN for the load cells. The data logger was linked to an PC and operated using the proprietary software, Scorpio through Windows. This package allowed the live plotting of the data during each test. Subsequently, the logged data in the hard disk was processed using the software package Excel through Windows.

7.8 Material testing

7.8.1 Reinforcement

For the stability tie bars for each test, two T25 × 1000 mm long hot-rolled deformed high tensile bars were cut at random from the lengths used in the tests. They were tested in accordance with the requirements of BS EN 10 002-1: 1990 for the yield stress and elastic modulus in the 2000 kN INSTRON 8500 testing machine. Results for test series are presented in Table 2.

7.8.2 Concrete

Compressive strength tests (to BS 1881, Part 116) were carried out on 100 mm size cubes which were cast simultaneously with the beam and column specimens, and with the infill concrete. The strength of the latter was used to dictate the testing date. All results are shown in Table 3.

Table 2 Test results of the 25 mm stability tie bars used in the tests carried out

Test ref.		Length of bar L (m)	Weight of bar M (gm)	Area of bar A (mm^2)	E_s (kN/mm^2)
TW1(A)	Bar A	1.000	3777	481	197.966
	Bar B	1.000	3792	483	202.936

Table 3 Test results of the 25 mm stability tie bars used in the tests carried out (continuous)

Test ref.		Yield load P_y (kN)	Yield stress f_y (N/mm^2)	Tensile load T (kN)	Tensile stress f_t (N/mm^2)
TW1(A)	Bar A	263.007	546.792	312.199	649.062
	Bar B	263.904	546.385	314.472	651.080

Table 4 Specified and average compressive cube strengths in test series 1

Member	Specified cube (28 day) strength (N/mm^2)	Actual cube strength (N/mm^2) (at testing)		
		TW1(A)	TW1(B)	TW1(C)
Column	40	56.3	56.3	56.3
Beam 1	40	54.9	54.9	54.9
Beam 2	40	50.4	50.4	50.4
Beam/column joint	40	45.4	45.4	45.0
Slab/beam/column/joint	30	33.8	33.8	N/A

7.9 Test monitoring and loading history

Each test was monitored by the live plotting of the applied bending load versus crack opening, beam-to-column joint compressive deformation, and concrete and steel strains. The performance of the connection was viewed on a PC monitor using the live results during the loading.

The loading scheme was aimed at simulating the cyclic action of the gravity force on a precast concrete skeletal frame. This action causes hogging bending moment to the beam-to-column connections.

At the beginning of the tests, the first recording scan was taken soon after the slab units' temporary supports were removed. The aim of this scan was mainly to record the initial bending load at the free end of the beams due to the self-weight of the test specimens. The second scan was taken as soon as the load cells used at the underneath of the free ends were removed to record the initial deflections.

The bending load was applied in four reversible cycles prior to loading monotonically to failure. The cyclic tests were performed to measure reductions in stiffness with increasing damage. The first three cycles (three cycles were chosen as being the least number) were applied in increments of 5 kN up to 30% (Mahdi 1992 showed major changes in behaviour at about 30% of ultimate load or moment) of the predicted failure load (see later Fig. 18). The fourth cycle was applied to 50% of the load with 10 kN load increment (see later Fig. 18). At the end of each cycle, at load zero level (load off), a scan was taken to calculate permanent deflections. When the monitored deflections indicated the onset of non-linearity, the load increments were reduced from 20 to 10 then 5 kN in the last cycle. Between any two successive increments a visible check was carried out on cracks in the critical zones of the sub-frame, and the stroke of the POTs and jacks. Where these were exceeded a scan was taken and the appropriate POT was reset followed by a further scan and the resumption of the loading.

It was decided to measure the flexural stiffness of the connections at the bending moment in the connections at the face of the column M_{con} ranging from 30 and 50 per cent of the M_{pred}. These limits have also been used at Tampere University of Technology (Finland). Because the stiffness decreases with an increase in moment, the moment at which the stiffness has been determined should always be stated. Repeated loading and unloading reduces the effect of the tensile stiffness of the floor slabs where cracks occur at low loads and give an artificially low stiffness so that the moment-rotation curve on second, third, fourth and final loading exhibits only small curvature.

The test procedure was to apply load increments until the joints were not capable of supporting any further bending load.

8. Results

8.1 Calculation of moment-relative rotation and stiffness

8.1.1 Calculation of moments

The applied hogging bending moment in the connection M_{con} at the face of the column, where the most critical zone of the connection is located due to the maximum bending stresses, was calculated by multiplying the magnitude of applied bending load P, recorded by the load cells 1 and 2 for the beams 1 and 2 respectively (Fig. 13), by the lever arm in the beam. This was considered constant at 2.365 m between the line of action of the applied loads at the ends of the beams and the faces of the column.

The initial bending moment of the connection M_i due to self-weight of the components was calculated using the same lever arm and the magnitude recorded by load cells 3 and 4 (Fig. 17) after removing the wedges of the slab units. M_i values were 6.80 and 6.45 kNm for beams 1 and 2, respectively in test TW1(A). These were ignored to be on conservative side and not involved in calculating actual (test) values of the joint M_{con} or M_u and not measured in the rest of the tests.

8.1.2 Calculation of relative rotations

The relative rotations ϕ between beam and column were calculated using two methods as follows:-

Method 1 (M1): Using vertical POTs mounted on two steel rods bolted to the column as shown in Fig. 17. They measured the vertical deflections (e.g., “POT14” means the deflection measured by POT no 14) of the beams and joints relative to the column including shear effects. Shear deflections are thus eliminated. The deflection divided by their respective distances (actual distances) from the column faces produced the required relative rotations as follows:-

For the beam 1 (B1) side:-

$$M1\ B1\ V1{:}\ \phi = \left(\frac{POT14}{90}\right) \tag{3}$$

$$M1\ B1\ V2{:}\ \phi = \left(\frac{POT16}{110}\right) \tag{4}$$

$$M1\ B1\ V3{:}\ \phi = \left(\frac{POT18}{300}\right) \tag{5}$$

$$M1\ B1\ V4{:}\ \phi = \left(\frac{POT18 - POT16}{300 - 110}\right) \tag{6}$$

Ditto for the beam 2 (B2) side.

Method 2 (M2): Using the horizontal POTs clamped to the top of the slab in-situ concrete and near to the top and bottom of the beams. They were clamped by drilling the slab in-situ, beams and column. They measured the crack openings δ_T and compressive deformations δ_B in the joints relative to the column (see Fig. 17). This method assumes full shear interaction between the floor slab and the beam. This method has also been used by Han *et al*. (2016). The required relative rotations were produced as follows:-

For the slab 1 (S1) and beam 1 (B1) side:-

$$M2\ S1{:}\ \phi = \left(\frac{\delta_T + \delta_B}{500}\right) = \left(\frac{POT2 + POT10}{500}\right) \tag{7}$$

Where

δ_T (mm) is the crack opening at the top of the slab 1 recorded by POT2.

δ_B (mm) is the compressive deformation in the joint recorded by POT10.

500 (mm) is the actual vertical distance between strokes of POT2 and POT10.

$$M2\ B1{:}\ \phi = \left(\frac{\delta_T + \delta_B}{260}\right) = \left(\frac{POT6 + POT10}{500}\right) \tag{8}$$

Where

δ_T (mm) is the crack opening at the top of the beam 1 recorded by POT6.

260 (mm) is the actual vertical distance between strokes of POT6 and POT10.

Ditto for the slab 2 (S2) and beam 2 (B2) side.

The rotations ϕ were then used in the presentation of the moment-relative rotation ($M_{con} - \phi$) graphs. The side-sway of the column in and out of the plane of bending were ignored due to the symmetrical loading of the beams, equal span slabs and the way of measuring deflection, because the POTs measured the deflections relative to the column itself.

8.1.3 Calculation of stiffnesses

The rotational stiffnesses, J (general), were calculated from the slope of the $M_{con} - \phi$ curve on the basis of both tangent stiffness and the secant stiffness of the chord of the curve. Each loading and unloading curve was analysed using regression analysis. Cycle 1 has five different estimates of rotational stiffness J as follows (see Fig. 18):

(a) Before cracking
  (1) The initial tangent flexural stiffness J_u, which is the slope of the $M_{con} - \phi$ curve from the beginning of the test to the first crack moment of the connection M_{cr}.

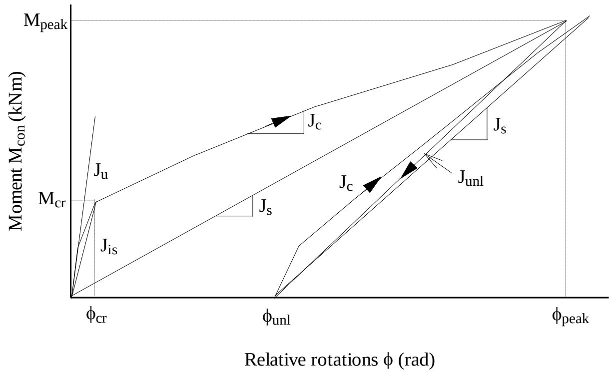

Fig. 18 Actual moment versus relative rotation curve at which flexural stiffnesses were defined for cycles 1-2

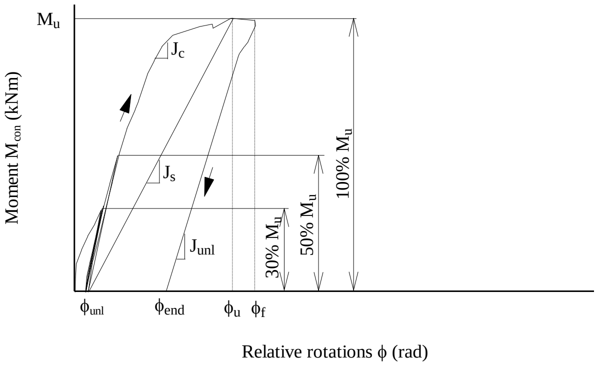

Fig. 19 Actual moment versus relative rotation curve at which flexural stiffnesses were defined for cycle 5

(2) The initial secant flexural stiffness J_{is}, which is the slope of the chord of the same curve in (1)
(3) b) After cracking
(4) The tangent flexural stiffness J_c, which is the slope of the $M_{con} - \phi$ curve from the M_{cr} to the peak moment of the cycle M_{peak}.
(5) The flexural stiffness of unloading curve J_{unl}.
(6) The secant flexural stiffness J_s, which is the slope of the chord of the $M_{con} - \phi$curve from the beginning of the cycle to the M_{peak}.

For the second, third and fourth cycles J_c and J_s were calculated from the beginning of reloading $M_{con} - \phi$ curves to the peak moment of the corresponding cycle M_{peak}. For the last cycle, C5, J_c was calculated up to a moment value at which the slope of the graph decreased rapidly (see Fig. 19).

8.2 Presentation of results

The results are presented from derived calculations. These include hogging bending moment in the connection M_{con} at the faces of the column versus crack opening δ_T at boundaries between the slabs and column and between the beams and column in the case of the test incorporating floor slabs and in-situ concrete, and between the beams and column only in the case of the test TW1(C). Moment versus compressive deformations δ_B in the joints, concrete and steel strains $\mu\varepsilon$, and relative rotations ϕ of the joints are also presented graphically. Where necessary the behaviour during the loading cycles 1-3 is enlarged and presented separately before each of the corresponding results to failure. The latter do not show the unloading cycles and are derived by the sequential superposition of peak values. This enables a full picture of the behaviour to be realised.

Figs. 20-21 represent the moment M_{con} versus crack opening δ_T, at boundaries of slabs and column, and beams and column, and M_{con} versus compressive deformations δ_B in the beam-to-column joints for the double sided

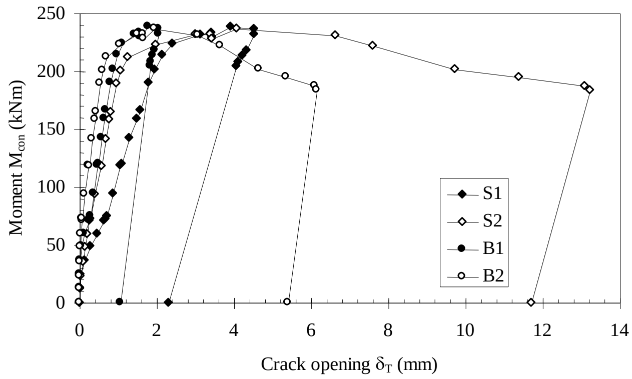

Fig. 20 Moment versus crack opening at slab/column and beam/column boundaries

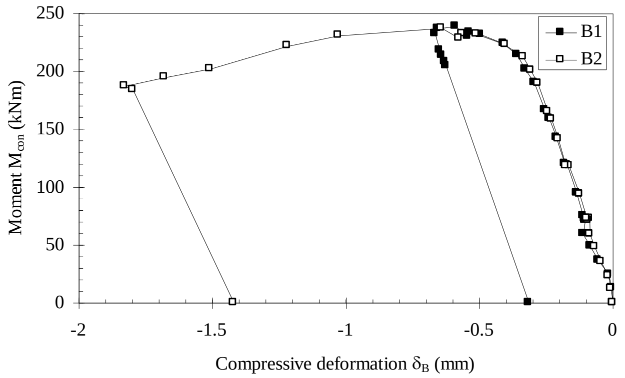

Fig. 21 Moment versus compressive deformation in joints

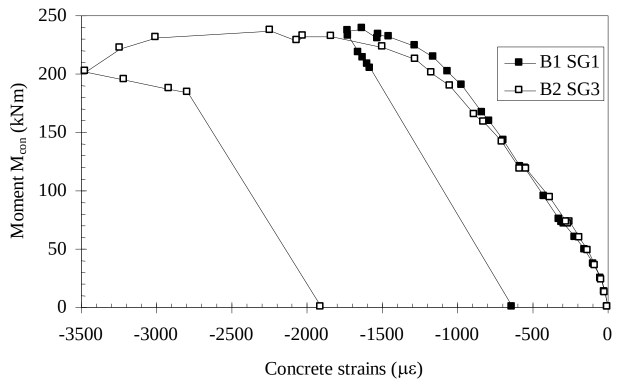

Fig. 22 Moment versus concrete strains in beams

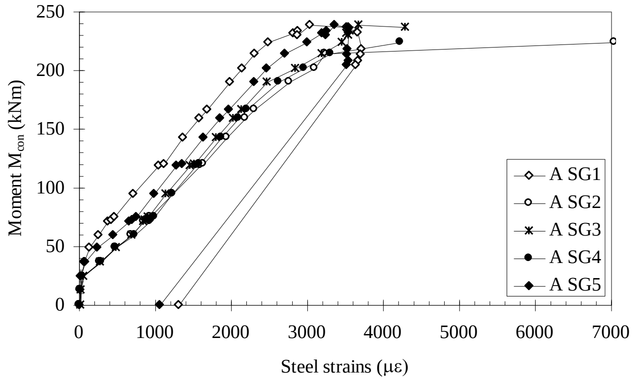

Fig. 23 Moment versus steel strains in bar A

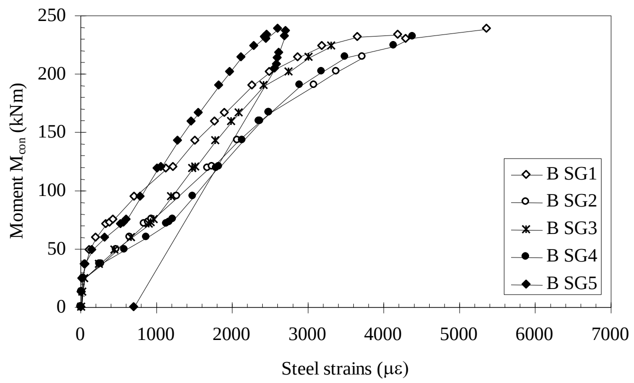

Fig. 24 Moment versus steel strains in bar B

welded plate connection. These results show the relative displacements which induces the relative rotations between the slabs and column, and the beams and the column. The displacements are a measure of the elastic and plastic deformation of the connection as a whole and represent a release in concrete strain in tension, which increases steel strains at the cracked section, the compressive strain generally, and strain in the joint concrete particularly.

Calculated moment versus concrete strains in compression in the precast beams, and steel strains in bars A and B are presented in Figs. 22 and 24, respectively. They define limits of the strains in the joint zone.

Fig. 25 shows vertical displacement profiles along each of the beams for selected values of moment in cycle 5 only. The gradients of these plots enable beam-to-column rotation to be derived using the Method 1. POTs 12 and 14 were used to record the vertical deflection of the joint that would give relative rotation of the joint to the column face, the POTs 16 and 18 recorded the vertical deflections of the beam 1. The rotation obtained from the gradient of these two POTs (not effected by the shear deformation) would give the relative rotation of the beam-to-column by dividing the relative deflections of the sensors by their relative offsets. This is the relative rotation commonly used in many computer programs by ignoring the length of the joint element and assuming the rotation of the joint takes place at its centre which varies according to the type of the connection, i.e., 50 mm from the face of the column for welded and 60 mm for the billet connection. The total

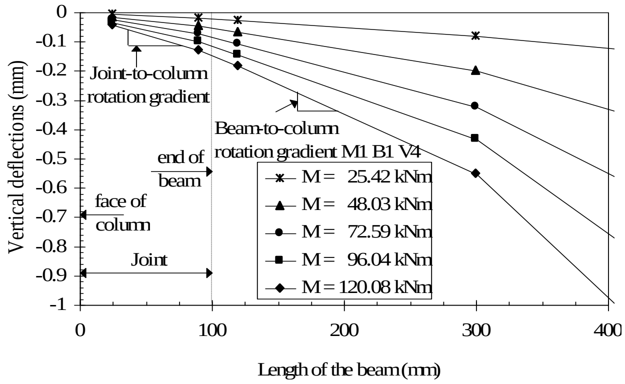

Fig. 25 Moment versus vertical deflections in beam 1 with various moment level

relative rotation does not include the curvature of the beam, the location of POTs 17 and 18 were 200 mm from the end of the beams which is less than the overall depth of the beam (h = 300 mm).

The derived moment versus relative rotation graphs obtained from the two methods are presented in Figs. 27 and 29.

Typical damaged zones for this test are presented in Figs 30-31. The notation refers to applied target increment load P in kN. It was convenient to mark cracks at the applied

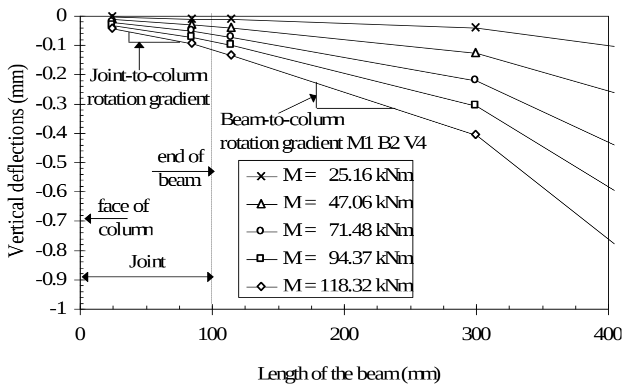

Fig. 26 Moment versus vertical deflections in beam 2 with various moment level

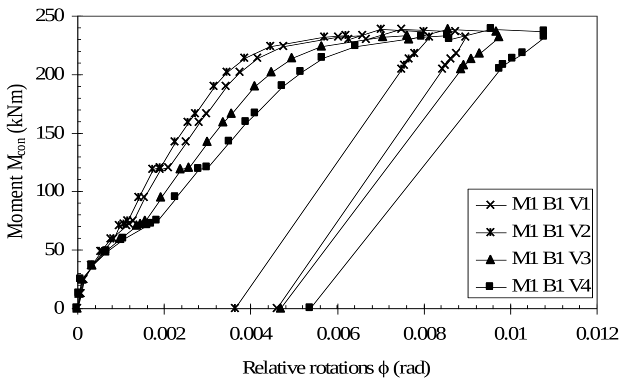

Fig. 27 Moment versus relative rotations in beam 1 using method 1

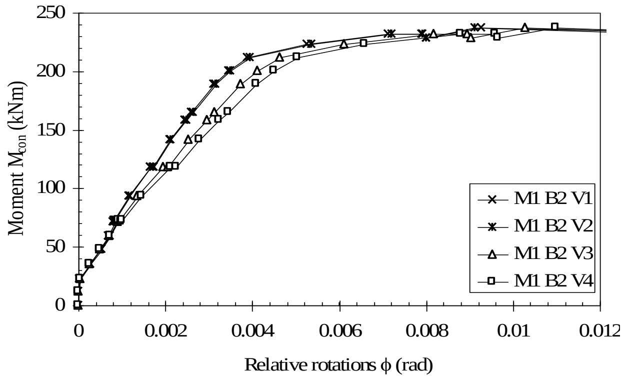

Fig. 28 Moment versus relative rotations in beam 2 using method 1

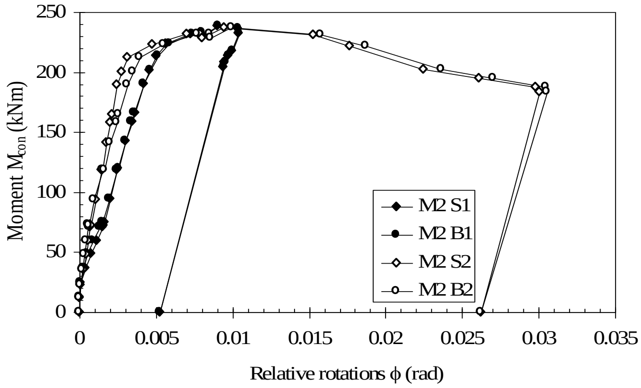

Fig. 29 Moment versus relative rotations using method 2

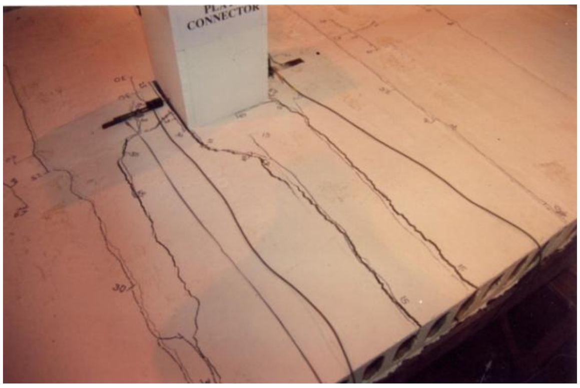

Fig. 30 Failure region at top of slab (Görgün 1997)

target increment load *P* they observed during the tests. It is important to note that (a) the recorded *P* values are slightly different from the marked P values, i.e., the above marked *P* = 15 kN has been recorded as 15.5 kN for beam 1 and 15 kN for beam 2, (b) the actual *P* values at which the cracks appeared are in between two recorded increments. This means that the marked values are the upper limits for the cracks. The first crack appeared at the column face and spread to the outer edge of the hollow core slab. Fig. 31 shows the damaged area of the joints. A circle has been drawn around the bottom right hand corner of the joint (Fig. 31) to indicate the extent of the concrete compression zone

Fig. 31 Failure region of beam-to-column joint

Table 5 Summary of test results

Test ref.		C1		C2	C3	C4	C5
		M_{cr} (kNm)	M_{peak} (kNm)	M_{peak} (kNm)	M_{peak} (kNm)	M_{peak} (kNm)	M_u (kNm)
TW1(A)	Beam 1	24.59	71.13	72.36	75.00	118.72	238.78
	Beam 2	23.05	72.28	71.24	72.65	118.38	237.01

Table 6 Summary of test results (continuous)

Test ref.		M_{pred} (kNm)	M_{beam} (kNm)	$\frac{M_{cr}}{M_u}$	$\frac{M_u}{M_{pred}}$	$\frac{M_u}{M_{beam}}$
TW1(A)	Beam 1	252.58	340.28	0.10	0.95	0.70
	Beam 2	252.58	338.01	0.10	0.94	0.70

and the final position of the neutral axis, i.e., about 100 mm from the bottom of the beam. Horizontal bursting cracks are a clear indication of unconfined concrete compressive failure in the in-situ concrete infill. A second horizontal crack occurs at the level of the top surface of the solid steel billet, and is possibly indicative of local stress concentrations there. A summary of the test results is presented in Table 4. The actual (test) cracked moment M_{cr}, the peak moments of each cycle M_{peak} and ultimate moment capacity of the connection M_u, the actual (predicted) ultimate moment capacity of the connection M_{pred} and beam M_{beam}, the ratio of the actual cracked moment to the actual ultimate moment of the connection and ratio of the actual moment of the connection to those predicted are also presented.

9. Discussion of full scale frame connection tests

The main aim of the experimental work on full scale frame connection tests has been to identify the moment-relative rotation $M_{con} - \phi$ characteristics and to recognise the inherent flexural stiffness J of the most widely used beam-to-column connections in precast concrete structures in the UK. Secondary behavioural information included crack opening δ_T at the boundaries of the slab (in-situ)/column and beam/column, compressive deformation δ_B in the compression zone in the joints, strain in the tie bars in the tension zone and strain in the concretes in the compression zone. The results, presented before, are discussed here and additional interpretative information, such as the comparison of all the tests in terms of the above mentioned behavioural is given.

The results indicate major differences in the response of the single sided test to the symmetrical double sided versions. The moment capacities of the connections are given in Table 4. The double sided connections achieved full capacity because the tie steel in the floor slab is fully effective.

The results also show that at M_u the relative rotation ϕ_u = 10 to 15 mrad. for double sided connections.

The zone of influence is defined as that region where the effects of the connection influence the $M_{con} - \phi$ behaviour both in the beam and column. The zone of influence in the beam depends on the type of connection. For the welded plate type, changes in rotation were measured at 450 mm from the centre line of the column.

9.1 Overview of on the experimental work

The successful structural performance of precast concrete systems depends on the connection behaviour. The configuration of the connection affects the constructibility, stability, strength and flexibility of the structure. Furthermore, connections play an important role in the redistribution of forces as the structure is loaded.

Beam-to-column connections are essential to develop frame action in precast concrete buildings. The connections must develop sufficient strength to resist the applied loads and must have sufficient stiffness to limit the side-sway movement of the structure.

In this study, connections were examined for structural performance, as measured by forces and deflections from which the moment-rotation of the connections were calculated at the face of the column. Emphasis was placed on the behaviour of the connection subjected to gravity loading. Although seismic analyses were not performed, the connections were subjected to cyclic loading in order to observe their behaviour under reversed loading.

The action of the gravity and wind load on a building affects joint behaviour. The flexural strength and stiffness of the joint both affect sway of the columns and the moments transferred to connecting members such as beams and slabs.

In the case of the sub-frames tested, the simulated maximum gravity load applied at end of beam(s) induced moment in joints at the face(s) of column which are a measure of the moment transfer capacity of the joints.

The free ends of all beams and slabs in the experimental work were temporarily simply supported. Therefore, the shear forces at these locations in the beams, which were recorded by the load cells, are the actual applied bending forces from which the moments in the connections were calculated.

This load path has been defined as the global load path (Mahdi 1992). It indicates that the joint constitutes an integral member (with zero length in analytical studies, Gorgun and Yilmaz 2012) of the structure particularly in transmitting forces to other connecting members. The magnitude of these forces depending on the type of sub-frame (double or single sided) and particularly the type of the connection (welded plate or billet) affects the size of the damaged zones in the joint and precast concrete members.

In addition to the global load path, there is a local load path associated with the joint being tested.

Using the local force path concept, it was possible to formulate expressions for predicting moment capacity of the joints as presented in Table 4. Due to the simplified nature of these expressions, it is therefore to be expected that the predicted moment capacities (Table 4) will be different from the experimental values. In the majority of the test carried out these expressions served as an approximate indicator of the maximum force applied to the end of the beam(s).

The member sizes and reinforcement of the precast concrete column and beam and their strength were chosen such as to simulate an actual building frame environment.

9.2 Overview on the presentation of test results

The graphical outputs of moment versus crack opening, compressive deformation, concrete and steel strains, vertical deflections and, most importantly moment versus relative rotations are assembled for tests carried out involving the welded plate and billet connections in order to facilitate comparison of the response of the joints to the applied bending moment.

In the presentation of the joint moment-rotation characteristics, the initial moment-rotation of the joints due to the self-weight of the components was considered to be small.

Fig. 20 presents a comparison of the moment versus crack opening at top of slabs and beams in the double sided using welded plate connection.

In all the tests carried out flexural cracks were, as expected, first initiated at the column to joint interface at the top of the slab and the beam. This plane is therefore a plane of weakness due to the relative strength and stiffness of the two different materials in the joint and the beam.

A lower cover to the stability tie bars, longer span slabs and higher bond stiffness between the plate and the surrounding concrete could have reduced the value of the initial crack opening. The variation in the magnitude of crack opening can be attributed to the quality of the concrete and the method of placing the concrete as these affect the bond strength.

It can be seen (see Fig. 20) that the crack opening varies substantially in the region where the first flexural crack was induced in the connection.

A transverse flexural crack (Fig. 20) was first observed at an applied bending moment of M_{con} = 35.5 kNm corresponding a load of 15 kN. The recorded crack widths at this point were 0.131 and 0.085 mm on either side of the column. The largest cracks are, as expected, at the column to joint interface (Fig. 31). These initiated at a moment of 35.5 kNm which coincides with the large reduction in stiffness seen in Figs. 29-30 and may be interpreted as the point at which the section is cracked flexurally. With increasing rotation, the cracking became more widespread near the joints. The compressive and tensile stresses which the joint was not able to withstand led the crack to spread to larger areas around the joint, including the precast concrete beams. These cracks intensified in the zone, in the beam, at the soffit of the joint where they propagated horizontally indicating flexural overstressing resulting from the increased moment capacity of the joint. The column showed no sign of cracking. Apart from one or two minor deviations in the results the behaviour was generally anticipated with non-linear behaviour commencing at about 80 per cent of the ultimate moment, i.e., 190 kNm. Signs of compressive concrete failure in the bottom of the beam were evident (Fig. 31).

Compressive deformations δ_B (Fig. 21) were measured over a distance of 180 mm, i.e., 100 mm joint plus 40 mm precast beam and column. The maximum concrete strain calculated from these values is 0.0037, and being greater than 0.0035 ultimate strain at which concrete is normally assumed to crush explains the onset of failure at M_u. The 0.0037 strain including two interfaces between joint/column and joint/beam is greater than the compressive concrete strain 0.00347 recorded by the surface strain gauges in the beams near to the joint zone at failure (Fig. 22). One might say that $0.00347 \cong 0.0035$ when measuring concrete strains. It is true, but it indicates, however small, the effects of the presence of the interfaces. After the concrete in the tension zone failed to take any more tensile force, these were then taken by the tie bars which increased steel strains to more than 7000 (A SG2 in Fig. 23) and 5400 (B SG1 in Fig. 24), indicating significant yielding of the bars. Ultimate failure was due to significant yielding of the bars and concrete crushing failure in the joints.

The moment-relative rotation $M_{con} - \phi$ results in Figs. 27 and 29 show small variations in the different methods of measurement up to about M_{con} = 50 kNm, i.e., approximately 1/5 ultimate. The figures show the gradual deterioration in the stiffness soon after the cracks became widespread near the joints. This is because as the moment increased, this led to high compressive and tensile strain in the joint which resulted in cracking and spalling in the concrete and therefore a reduction in both the effective cross section area and the lever arm. The increase in the size of the cracked zone is an indication of the area of the plastification. A stage is reached where the joints are not able to withstand any more applied moment. At this stage the joint may be considered at its plastic moment of resistance M_u. Figs. 27 and 29 show that the moment-rotation behaviour is generally non-linear and the extent of the deviation from linearity is dependent on both the details of the connection and sub-frame. To this end, the scale of the moment-rotation curves reveal a great deal about the initial response of the joints, since the rotation is very small and therefore undetectable in the early stage of the loading history. Where necessary the behaviour during the loading cycles 1-3 is enlarged and presented separately before each of the corresponding results to failure to evaluate the initial behaviour. Therefore, the initial response of the moment-rotation results must be carefully interpreted. This is because in the majority of the moment-rotation graphs the joint might appear to have maintained full continuity of moment up to approximately 50% of the cracked moment M_{cr}. This could be attributed to the in-situ infill concrete which provided the initial tensile stiffness.

The increase in the moment capacity in the case of test TW1(A) is mainly due to the presence of the slab continuity longitudinal bars. These not only satisfied the stability requirements of the BS 8110 (1985) but also increased the main characteristics, moment (by 215%), rotation (by 46%) and stiffness (by 105%) of the connection. Currently, in practice this remarkable contribution of the floor strength and stiffness to the flexural capacity of the joint is neglected in the design process of the precast concrete frames.

The incorporation of the slabs satisfied other structural requirements such as composite action with the beam, and slab continuity in tension across the beam/column zone. These structural improvements significantly influenced the global strength, stiffness and ductility of the sub-frame tested. As mentioned this test was terminated because of the significant yielding of the bars and concrete crushing failure in the joints. This indicates that the flexural continuity of the connection was being maintained to the extent that it weakened the bars and joint concrete. Thus flexural behaviour of test TW1(A) suggests that the slab could be idealised as a 200 mm deep beam acting compositely with the main 300 mm deep beam. It has been found by Mahdi (1992) that the out of plane dimensions of slab carry no structural significance other than imposing gravity forces on the beam.

At no point do the rotations obtained using Eqs. (6) and (8) differ by more than 8% and 13% of one another for beams 1 and 2, respectively. This gives greater confidence when using the “component method” based on the horizontal deflections from the isolated joint tests in Görgün (1997).

The horizontal deformations at the top of the beam were in linear relationship with δ_T and δ_B, showing that the beam and slab were rotating as a rigid block. These data also showed that the neutral axis for the flexurally cracked section was near to the level of the welded plate connection. An exact agreement was obtained between the rotations derived using M2 S1 and M2 B1 (see Fig. 29). This shows that, within the normal scatter experimental work of this type, either method may be used to generate $M_{con} - \phi$ data, and is the first step towards the validation of the “component method” (Görgün 1997).

The lowest tangent flexural stiffness, J_c = 45,800 kNm/rad. (M1 B1 V4), is obtained using Method 1, compared with values of about J_c = 50,000 kNm/rad. (M2 S1) and J_c = 49,500 kNm/rad. (M2 B1) using Method 2. It is for this reason that all subsequent results and design values will be based on Method 1 V4 (see Eq. (6)).

The tangent and unloading stiffnesses of the connection for Beam 2 (Method 1) is always greater than the Beam 1 because of more cracks on Beam 1 side (see Fig. 30). The tangent stiffnesses decrease very rapidly due to the first flexural tensile (transverse) cracks occurring at low loads and gave low stiffness in cycle 1. These cracks reduced the contribution of the tensile stiffnesses of the slabs to the stiffnesses of the connections. Repeated loading and unloading in cycle 2 reduced this effect, hence increased the stiffnesses of the connections. There is no significant change in stiffnesses in cycle 3. The stiffness decreased in beam 2 side in cycle 4, because the stiffness decreases with an increase in moment and damage in the previous cycles and came close to the stiffness in beam 1 side. This is an indication of the failure to take place at Beam 2 side.

In addition to the above observations, the stiffnesses obtained from the slab rotations (Method 2) are less than those obtained from the beam rotations in the cycles 1-3, unlike in the cycles 4-5 as a result of more cracks far from the column faces giving less crack opening at column/slab (in-situ) boundaries. By comparing the results of the two Methods it is found that the Method 1 gives a lower tangent stiffnesses than the Method 2 in each cycle for both beams and joints.

The mean ultimate moment M_u value 237.90 kNm, ultimate rotation ϕ_u = 10.3 and 9.5 mrad and secant stiffness J_s = 25450 and 27100 kNm/rad were achieved in this test using Methods 1 and 2, respectively. The value 0.70 × the actual ultimate moment capacity of the composite beam M_{beam} was attained. Currently, in practice this remarkable contribution of the strength and stiffness to the flexural capacity of the precast concrete members is neglected in the design process of the precast concrete frames.

10. Conclusions

The current practice in the design of precast concrete frames is to ignore any inherent strength, stiffness and ductility existing in the connections between the beams and columns, and to design both beams and columns on the assumption of pinned joints. The effect of this on the design of sway frame columns results in impracticable and uneconomical selections for frames above three stories. This is because the column is assumed to behave as a vertical cantilever from the foundation transferring all the beam reaction moments and wind moments in an additive manner fully to the base without involving frame action. For larger columns the additional moments due to $P - \Delta$ and instability effects become prohibitive.

The presence of concrete as grout-filled joints is ignored in design except to protect the mechanical connection from corrosion and fire danger. Similarly, the presence of longitudinal reinforcing bars interconnecting the beam and column at floor level for frame integrity purposes is not utilized, in other ways in current design procedures. However, it is clear that the presence of such existing materials together with that of the mechanical connection, must provide the joint with existing residual strength, stiffness and ductility properties which are at present untapped.

The work developed in this study builds on the previous promising work in the field at Nottingham University which indicated the positive design and behavioural advantages of utilising the existing semi-rigid joint properties which allow for the safe design of such structures in the form of small slender columns for taller structures.

The present work advances the knowledge base in the following ways:-

(1) Full scale of testing of double sided welded plate and the billet connections, has showed that the essential $M - \phi$ relation could be assessed in several independent ways. This has been done for the beam/column alone, beam and floor slab/column composite behaviour for double sided beam arrangements. This has given a more complete data base of the semi-rigid joint behaviour, including various elastic stiffnesses which could be incorporated into design.

(2) A fundamental appraisal of the behaviour of in-situ joint concrete surrounded by stirrups precast concrete, resulting in a new estimate of strength and stiffness, depending on the relative thickness of the in-situ bond has been established, which can be used to simulate concrete compression joint behaviour.

The frame connection test showed that damage to the precast sub-frame occurred mainly at the bottom of the connections in the compression zone whilst the members had suffered little damage beyond the connections. The initial tangent flexural stiffness of the connection was maintained up to 0.10 to 0.13 of the ultimate moment capacity of the connection M_u in the double sided connections tests. At failure M_u was approximately 0.84 to 0.95 of the predicted ultimate moment of resistance of the connections in double sided tests. The effect of the floor slab and the tie bars was to increase the ultimate moment (by 215%), stiffness (by 105%) and rotation (by 46%) compared to the basic connection. Currently, in practice this remarkable contribution of the floor strength and stiffness to the flexural capacity of the joint is neglected in design.

The most important conclusion from this study is that the double –sided connections achieved full capacity because the site –placed tie steel in the floor slab is fully effective, and the connection may therefore, be appropriately used in a semi-rigid frame design.

Acknowledgments

The research described in this paper was financially supported by the Engineering and Physical Sciences Research Council (EPSRC) in the United Kingdom, and the Turkish Government.

References

ACI 318 (2014), Building code requirements for structural concrete and commentary; American Concrete Institute, Farmington Hills, MI, USA.

Anderson, D., Colson, A. and Jaspart, J.P. (1993), “Connections and frame design for economy", *New Steel Construction*, 30-33.

Bhatt, P. and Kirk, D.W. (1985), "Tests on improved beam-to-column connections for precast concrete", *ACI Journal*, **82**(6), 835-843.

BS 5950 (1985), The Structural use of steelwork in building, British Standards Institute; London, UK.

BS 8110 (1985), The structural use of concrete, British Standards Institute; London, UK.

BS EN 10 002-1: (1990): Part 1: Tensile testing of metallic materials, Method of test at ambient temperature.British Standards Institute; London, UK.

Chefdebien, A. and Dardare, J. (1994), **"**Experimental investigations on current connections between precast concrete components", *COST C1 Proceedings of the 2nd Workshop, Semi-rigid Behaviour of Civil Engineering Structural Connections*, Prague, Czech Republic, October.

Cheok, G.S. and Lew, H.S. (1991), "Performance of precast concrete beam-to-column connections subject to cyclic loading", *PCI Journal*, **36**(3), 56-67.

Cheok, G.S. and Lew, H.S. (1993), "Model precast concrete beam-to-column connections subject to cyclic loading", *PCI Journal*, **38**(4), 80-92.

Cheok, G.S., Stone, W.C. and Kunnath, S.K. (1998), "Seismic response of precast concrete frames with hybrid connections", *ACI Struct. J.*, **95**(2), 527-539.

Choi, H.K., Choi, Y.C. and Choi, C.S. (2013), "Development and testing of precast concrete beam-to-column connections", *Eng. Struct.*, **56**, 1820-1835.

Comair, F. and Dardare, J. (1992), "Model testing of precast semi-rigid beam-column connection", *Proceedings of the First State of the Art Workshop, COST C1*, Strasbourg, France, October.

Demartino, C., Monti, G. and Vanzi, I. (2017), "Seismic loss-of-support conditions of frictional beam-to-column connections", *Struct. Eng. Mech., Int. J.*, **61**(4), 527-538.

Dolan, C.W. and Pessiki, S.P. (1989), "Model testing of precast concrete connections", *PCI Journal*, **56**(2), 85-103.

Dolan, C.W., Stanton, J.F. and Anderson, R.G. (1987), "Moment resistant connections and simple connections", *PCI Journal*, **32**(2), 62-74.

Elliott, K.S. (2017), *Precast Concrete Structures*, (2nd Edition), Boca Raton: Taylor & Francis Group, CRC Press, New York, NY, USA.

Elliott, K.S., Davies, G., Gorgun, H. and Adlparvar, M.R. (1998), "The stability of precast concrete skeletal structures", *PCI Journal*, **43**(2), 42-60.

Elliott, K.S., Davies, G., Marcelo, F., Gorgun, H. and Mahdi, A.A. (2003a), "Can precast concrete structures be designed as semi-rigid frames? Part 1 - The experimental evidence", *Struct. Engr.*, **81**(16), 14-27.

Elliott, K.S., Davies, G., Marcelo, F., Gorgun, H. and Mahdi, A.A. (2003b), "Can precast concrete structures be designed as semi-rigid frames? Part 2 - Analytical equations and column effective length factors", *Struct. Engr.*, **81**(16), 28-37.

Englekrik, R.E. (1995), "Development and testing of a ductile connector for assembling precast concrete beams and columns", *PCI Journal*, **40**(2), 36-51.

Ertas, O., Ozden, S. and Ozturan, T. (2006), "Ductile connections in precast concrete moment resisting frames", *PCI Journal*, **51**(3), 66-76.

Eurocode 2 (2004), Design of Concrete Structures; European Committee for Standardization, Brussels, Belgium.

Gorgun, H. (1997), "Semi-rigid behaviour of connections in precast concrete structures", Ph.D. Thesis; University of Nottingham, Nottingham, UK.

Gorgun, H. and Yilmaz, S. (2012), "Geometrically nonlinear analysis of plane frames with semi-rigid connections accounting for shear deformations", *Struct. Eng. Mech., Int. J.*, **44**(4), 539-569.

Han, C., Li, Q., Wang, X., Jiang, W. and Li, W. (2016), "Research on rotation capacity of the new precast concrete assemble beam-column joints", *Steel Compos. Struct., Int. J.*, **22**(3), 613-625.

I Struct E Manual (1978), Structural joints in precast concrete, The Institution of Structural Engineers; Manual. 11 Upper Belgrave Street, London, UK.

Kataoka, M.N., Ferreira, M.A. and El Debs, A.L.H.C. (2015), "Study on the behavior of beam-column connections in precast concrete structure", *Comput. Concrete, Int. J.*, **16**(1), 163-178

Khaloo, A.R. and Parastesh, H. (2003), "Cyclic loading of ductile precast concrete beam-column connection", *ACI Struct. J.*, **100**(4), 291-296.

Kulkarni, A.S. and Li, B. (2009), "Investigations of seismic behaviour of hybrid connections", *PCI Journal*, **54**(1), 67-87.

Kulkarni, A.S., Li, B. and Yip, W.K. (2008), "Finite Element analysis of precast hybrid-steel concrete connections under cyclic loading", *J. Construct. Steel Res.*, **64**(2), 190-201.

Kwong, Y.W. and Teng, S. (2000), "Hybrid precast concrete beam", *CSE Research Bulletin*, No. 13, pp. 78-80.

Li, B., Kulkarni, A.S. and Leong, C.L. (2009), "Seismic performance of precast hybrid-steel concrete connections", *J. Earthq. Eng.*, **13**(5), 667-689.

Loo, Y.C. and Yao, B.Z. (1995), "Static and repeated load tests on precast concrete beam-to-column", *PCI Journal*, **40**(2), 106-115.

Mahdi, A.A. (1992), "Moment-rotation behaviour of connections in precast concrete structures", Ph.D. Thesis; University of Nottingham, Nottingham, UK.

Marsono, A.K., Ying, W.J., Tap, M.M., Chieh, Y.C. and Haddadi, A. (2015), "Standard Verification Test for Industrialised Building System (IBS) Repetitive Manufacturing", *Procedia CIRP*, **26**(2015), 252-257.

Moghadasi, M. and Marsono, A.K. (2012), "Comparative experimental study of full-scale H-subframe using a new industrialized building system and monolithic reinforced concrete beam-to-column connection", *Struct. Des. Tall Special Build.*, **23**(8), 563-579.

Moghadasi, M., Marsono, A.K. and Mohammadyan-Yasouj, S.E. (2017), "A study on rotational behaviour of a new industrialised building system connection", *Steel Compos. Struct., Int. J.*, **25**(2), 245-255.

Mohamed, S.A.M. and Jolly, C.K. (1995), "An experimental study of the behaviour of sleeved bolt connections in precast concrete frames", *Magaz. Concrete Res.*, **47**(171), 119-127.

Pillai, S.U. and Kirk, D.W. (1981), "Ductile beam-column connection in precast concrete", *ACI Journal*, **78**(6) 480-487.

Rahman, A.B.A., Hock, L.J., Saim, A.A. and Osman, M.H. (2007), "Design and testing of a full scale precast concrete h-subframe", *Proceedings of the 1st Construction Industry Research Achievement International Conference* (*CIRAC2007*), Kuala Lumpur, Malaysia, March.

Stanton, J.F., Anderson, R.G., Dolan, C.W. and Mc Cleary, D.E. (1986), "Moment resistant connections and simple connections", PCI Specially Funded Research and Development Program, Research Project 1/4 Prestressed Concrete Institute, Chicago, IL, USA.

Seckin, M. and Fu, H.C. (1990), "Beam-column connections in precast reinforced concrete construction", *ACI Struct. J.*, **87**(3), 252-261.

Virdi, K.S. and Ragupathy, P. (1992), "Tests on precast concrete subframes with semi-rigid joints", *Proceedings of the First State of the Art Workshop, COST C1*, Strasbourg, France, October.

Yang, K.H., Oh, M.H., Kim, M.H. and Lee, H.C. (2010), "Flexural behaviour of hybrid precast concrete beams with H-steel beams at both ends", *Eng. Struct.*, **32**(9), 2940-2949.

Zoubek, B., Isakovic, T., Fahjan, Y. and Fischinger, M. (2013), "Cyclic failure analysis of the beam-to-column dowel connections in precast industrial buildings", *Eng. Struct.*, **52**, 179-191.

CC